

AD-A247 588



2
AWS/TN--91/001



**DUST AND SAND FORECASTING
IN IRAQ
AND ADJOINING COUNTRIES**

by

**MSGT WALTER D. WILKERSON
AFGWC/DOF**

NOVEMBER 1991

**DTIC
ELECTE
MAR 12 1992
S B D**

**APPROVED FOR PUBLIC RELEASE;
DISTRIBUTION IS UNLIMITED**

92 11 008

92-06500

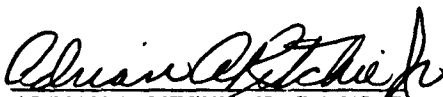


**AIR WEATHER SERVICE
Scott Air Force Base, Illinois 62225-5008**

BEST AVAILABLE COPY

REVIEW AND APPROVAL STATEMENT

AWS/TN--91/001, *Dust and Sand Forecasting in Iraq and Adjoining Countries*, November 1991, has been reviewed and is approved for public release. There is no objection to unlimited distribution of this document to the public at large, or by the Defense Technical Information Center (DTIC) to the National Technical Information Service (NTIS).



ADRIAN A. RITCHIE, JR., Col, USAF

Director of Technology

Air Weather Service

FOR THE COMMANDER



WALTER S. BURGMANN

Scientific and Technical Information

Program Manager

29 November 1991

A NOTE TO OUR CUSTOMERS--

The authors and editors of this publication welcome feedback, both positive and negative. We value your opinion. Please let us know what you like and do not like about our products. Also, please let us know if your address has changed, or if you wish to receive more or fewer copies of AWS and USAFETAC technical documents in primary distribution. If you need more copies of this document, or if you know of someone else who might be interested in this or other AWS/USAFETAC publications, let us know that, too. Call, write, or FAX:

USAFETAC/LDE,
Scott AFB, IL 62225-5458

DSN 576-6648 Commercial 618 256-6648 FAX 3772

REPORT DOCUMENTATION PAGE

2. Report Date: November 1991
3. Report Type: Technical report
4. Title: Dust and Sand Forecasting in Iraq and Adjoining Countries
6. Author: MSgt Walter D. Wilkerson, AFGWC/DOF
7. Performing Organization Name and Address: Air Weather Service, Scott AFB (AWS/XTX), IL 62225-5008
8. Performing Organization Report Number: AWS/TN--91/001
12. Distribution/Availability Statement: Approved for public release; distribution is unlimited.
13. Abstract: This report, based partly on the author's recent personal experience in desert weather forecasting, discusses airborne dust and sand in Iraq, Kuwait, Syria, eastern Jordan, western Iran, and the northern Arabian Peninsula. Describes geography of the region and discusses general types of duststorms and sandstorms. Locates and describes sources of sand and dust in Mesopotamia, Southwest Asia, and the Red Sea area. Provides practical tips and rules of thumb for forecasting airborne sand and dust. Describes methods for enhancing the appearance of airborne dust in satellite imagery and provides example satellite imagery that shows airborne dust produced under several conditions.
14. Subject Terms: METEOROLOGY, WEATHER, WEATHER FORECASTING, LITHOMETEORS, SAND, DUST, SANDSTORM, DUSTSTORM, SUSPENDED DUST, DUST HAZE, METEOROLOGICAL SATELLITES, SATELLITE PHOTOGRAPHY, SATELLITE IMAGERY, MIDDLE EAST
15. Number of Pages: 72
17. Security Classification of Report: Unclassified
18. Security Classification of this Page: Unclassified
19. Security Classification of Abstract: Unclassified
20. Limitation of Abstract: UL

Accession For	
NTIS CRA&I	<input checked="" type="checkbox"/>
DTIC TAB	<input type="checkbox"/>
Unannounced	<input type="checkbox"/>
Justification	
By	
Distribution/	
Availability Codes	
Dist	Avail and/or Special
A-1	

Standard Form 298

PREFACE

The effects of blowing dust and sand have long been recognized as having a major influence on military operations. A book published in Great Britain during World War II, for example, noted that the presence of large-scale military operations in the Sahara and the loosening of the desert surface had increased the likelihood of duststorms considerably (NAVENVPREDRSCHFAC, 1980). A U.S. Army manual states that "dust and sand in the air may be the single most destructive environmental element to military equipment" (Hook, 1984).

A great deal of information on airborne dust and sand has been published in periodical literature, most during the last 20 years. This report uses that information, along with the author's personal experience in the desert, to produce what we hope to be a comprehensive and useful handbook on the subject.

The area to be discussed here includes Iraq, Kuwait, Syria, eastern Jordan, western Iran, and the northern Arabian Peninsula. Part 1 discusses the geography of the study area and touches on seasonal climatology. Part 2 describes the major types of duststorms that occur across the Middle East. Part 3 gives specific source areas from which dust and sandstorms originate. Part 4 provides some duststorm forecasting tips and rules of thumb. Part 5 discusses methods available for enhancing the appearance of sand on satellite imagery, while Parts 6-11 provide actual examples of satellite imagery showing airborne dust and sand.

CONTENTS

	Page
Chapter 1 Geography	1
1.1 The Study Area Defined and Described	1
1.2 Water Features	1
1.3 Maps	1
Chapter 2 Major Duststorm Types	4
2.1 Shamal	4
2.1.1 Summer Shamal	4
2.1.2 Winter Shamal	7
2.2 Frontal Duststorms	8
2.2.1 Prefrontal Duststorms	8
2.2.2 Postfrontal Duststorms	11
2.2.3 Shear-line Duststorms	11
2.3 Convective Duststorms	12
2.3.1 The Haboob	12
2.3.2 Dust Devils	13
Chapter 3 Duststorm Source Regions	15
3.1 Mesopotamian Region Duststorm Sources	16
3.2 Southwest Asia Duststorm Sources	19
3.3 Red Sea Area Duststorm Sources	21
Chapter 4 Dust Forecasting	23
4.1 Lifting Thresholds	23
4.2 Settling Thresholds	24
4.3 Effects of Particle Sizes	24
4.4 Rules of Thumb for Sand/Dust Forecasting	25
Chapter 5 Enhancing the Appearance of Dust in Satellite Imagery	28
5.1 Lithometeor Enhancement Curves for Orbiting Satellites	28
5.2 Composite Imagery	35
5.3 Histograms	35
Chapter 6 Example Satellite Imagery--The Winter Shamal	36
Chapter 7 Example Satellite Imagery--The Summer Shamal	42
Chapter 8 Example Satellite Imagery--Vortex	49
Chapter 9 Example Satellite Imagery--The Haboob	55
Chapter 10 Example Satellite Imagery--Mountain Gap	57
Chapter 11 Example Satellite Imagery--Other	58
BIBLIOGRAPHY	62

FIGURES

Figure 1-1.	The study area: Iraq and its neighbors	2
Figure 1-2.	Major water features in the area of interest.....	3
Figure 2-1.	Average climatic gradient-level windflow in July (Atkinson, 1971).....	4
Figure 2-2.	Typical dust plume life cycle	5
Figure 2-3.	How dust and sand travel	6
Figure 2-4.	Mean surface positions of the Monsoon Trough in July and August	7
Figure 2-5.	Average climatic gradient-level windflow in January (Atkinson, 1971).....	7
Figure 2-6.	Lawson's Density Current (A) and Compton's Turbidity Current (B).....	8
Figure 2-7.	Prefrontal and postfrontal kaus winds diagrammed.....	9
Figure 2-8.	Locations of stations corresponding to the numbers in Tables 4 and 5	10
Figure 2-9.	Atkinson's model of a surface shear line	11
Figure 2-10.	Comparisons of signatures in satellite imagery	12
Figure 2-11.	The formation of a haboob.....	13
Figure 2-12.	Wind recorder trace of dust devil at Holloman AFB, NM, 22 April 1976	14
Figure 3-1.	Mesopotamian template map	16
Figure 3-2.	Southwest Asia template map	19
Figure 3-3.	Red Sea Area template map	21
Figure 4-1.	Nomogram to be used for forecasting speed and height of the nocturnal jet. (Membery, 1983).....	27
Figure 5-1.	Example NOAA enhancement curve	28
Figure 5-2.	Original NOAA enhancement curve.....	29
Figure 5-3.	NOAA summer season curve.....	30
Figure 5-4.	Winter DMSP/summer NOAA	31
Figure 5-5.	NOAA transition season enhancement curve.....	32
Figure 5-6.	NOAA winter enhancement curve	33
Figure 5-7.	DMSP summer enhancement curve	34
Figure 6-1.	Blowing dust associated with a moderate cold front across the northern Persian Gulf and northeastern Saudi Arabia	36
Figure 6-2.	The blowing dust from Figure 6-1 is shown here 3 days later	37
Figure 6-3.	A strong cold-front-generated sandstorm can be seen moving from Iraq and northern Saudi Arabia toward the southeast	38
Figure 6-4.	The afternoon image of the strong spring cold frontal sandstorm shown in Figure 6-3.....	39
Figure 6-5.	The infrared (IR) version of Figure 6-4 shows both the extent of the dust and the cumulus formation better.....	40
Figure 6-6.	A normal IR shot across central Africa shows the extent of blowing dust/sand associated with the almost permanent winter shear line in this area	41
Figure 7-1.	Narrow plumes of dust are seen in the early stages of a summer shamal duststorm in southeastern Iraq	42
Figure 7-2.	The IR version of the image in Figure 7-1 detects the light colored plumes of dust in Iraq moving over the moister and darker shaded surface areas.....	43
Figure 7-3.	An afternoon light shot across the Arabian Peninsula showing the typical summer shamal plumes extending from southeastern Iraq to the south into Kuwait and the northern Persian Gulf	44
Figure 7-4.	The normal IR counterpart of the image in Figure 7-3	45
Figure 7-5.	The enhanced IR image of the previous two images (Figures 7-3 and 7-4)	46
Figure 7-6.	A sunset light pass shows a large-scale summer shamal duststorm at full strength	47
Figure 7-7.	An evening light pass showing a full-scale summer shamal duststorm in the eastern Arabian Peninsula	48
Figure 8-1.	A well-developed duststorm over the southeastern Arabian Peninsula is seen circulating into a low-pressure area in the Monsoon Trough.....	49
Figure 8-2.	A nighttime pass under a full moon creates some excellent visual imagery.....	50

Figure 8-3.	A sunrise expanded light shot of a large-scale duststorm that has circulated into a low-pressure area associated with the monsoon/thermal trough over the southeastern Arabian Peninsula.....	51
Figure 8-4.	An afternoon light image across northwestern Africa shows little or no visible dust, but an area of slightly lighter than normal shading can be seen on the west side of the image	52
Figure 8-5.	The normal IR counterpart of the image shown in Figure 8-4 shows a narrow band of blowing dust on the west side of the imagery	53
Figure 8-6.	The enhanced IR of the previous two images (Figures 8-4 and 8-5) further increases the amount of dust that can be seen	54
Figure 9-1.	Thunderstorms generated by a weak frontal system in Iraq have created a haboob-style duststorm in southeastern Iraq	55
Figure 9-2.	A light image over central Africa shows the size that downrush arcs can achieve.....	56
Figure 10-1.	Dense dust is seen blowing from Sudan through the Tokar Gap into the Red Sea.....	57
Figure 11-1.	A postfrontal enhanced IR image across the northern Arabian Peninsula	58
Figure 11-2.	An afternoon light image across northeastern Africa with no dust visible	59
Figure 11-3.	The normal IR counterpart of the image in Figure 11-2	60
Figure 11-4.	The enhanced IR version of the previous two images (Figures 11-2 and 11-3) increases the amount of dust visible	61

TABLES

TABLE 1.	Percentage frequencies of wind directions during dust disturbances at Baghdad (annual averages), 1950-1960 (Awad)	9
TABLE 2.	Percentage frequencies of wind speeds during dust disturbances at Baghdad (annual averages), 1950-1960 (Awad)	9
TABLE 3.	Average number of days with duststorms at Baghdad (Awad).....	9
TABLE 4.	Percentage frequencies of wind directions during dust occurrences at selected stations (annual averages), 1973-1989 (ISMCS, 1990).....	9
TABLE 5.	Average number of days of dust/sand at selected stations (ISMCS, 1990)	10

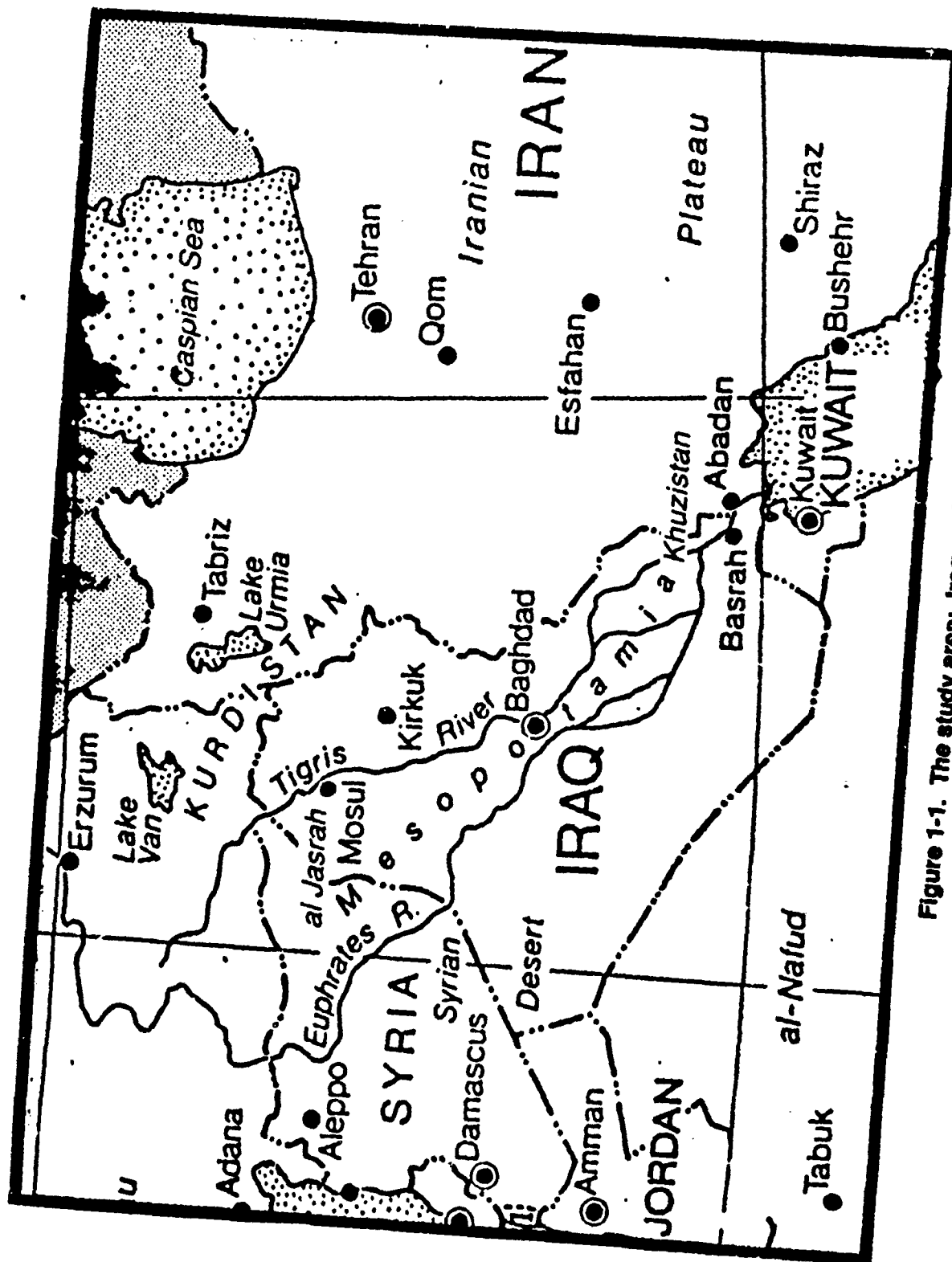


Figure 1-1. The study area: Iraq and its neighbors.

1. GEOGRAPHY

1.1 THE STUDY AREA DEFINED AND DESCRIBED

The area of the Middle East to be discussed here includes Iraq, Kuwait, Syria, eastern Jordan, western Iran, and the northern Arabian Peninsula. Figure 1-1 is a map of the study area, which shows the four major regions into which it is divided. The first of these, known as the "Syrian Desert," comprises that part of Iraq southwest of the Euphrates River, northern Saudi Arabia, eastern Syria, and eastern Jordan. This is primarily a "pebble desert," with little vegetation except along seasonal wadis (dry stream beds). That part of Iraq that lies between the Tigris and Euphrates Rivers northwest of the city of Baghdad is known as "al Jasrah" (or "Jazirah"), Arabic for "the island." East of the Tigris river in northeastern Iraq and northwestern Iran are the foothills of the Zagros Mountains; this region is known as "Kurdistan," for the large number of Kurdish people who have settled there. The last region lies in the southeastern tip of Iraq and includes the western plains of Iran just north of the Persian Gulf to the east of the Zagros Mountains; it is called "Khuzistan," for a province of Iran.

1.2 WATER FEATURES

Figure 1-2 gives the locations of rivers, lakes, and a few of the smaller mountain areas not associated with the Zagros Mountains. These lakes and rivers are prominent in visual satellite imagery and therefore instrumental in locating blowing dust and sand.

1.3 MAPS

A few good maps, with varying scales and differing degrees of resolution, are available for the region. Maps with higher resolution are available, but for normal use these are best. They are all available from the Defense Mapping Agency (DMA), 8613 Lee Highway, Fairfax, VA 22031-2137, DSN 287-2495, commercial 301 227-2495.

GNC 12 1:5,000,000 Middle East, Northeast Africa, South Asia. Excellent depiction of lava flows visible on satellite imagery over Saudi Arabia.

JNC 35 1:2,000,000 Middle East. Good depiction of wadis and regional lakes.

ONC H-6 1:1,000,000 South Iraq, West Iran, Northeast Saudi Arabia, Persian Gulf. Good terrain detail.

ONC G-4 1:1,000,000 North Iraq, Syria. Good terrain detail.

Another map (British) covers the Middle East in substantial detail and provides a superb look at regional geography even though the orientation is at a strange angle. It is published by Her Majesty's Stationery Office (HMSO), London, 1982. Ask for Series 1106, Sheet 3, Edition 5-GSGS.

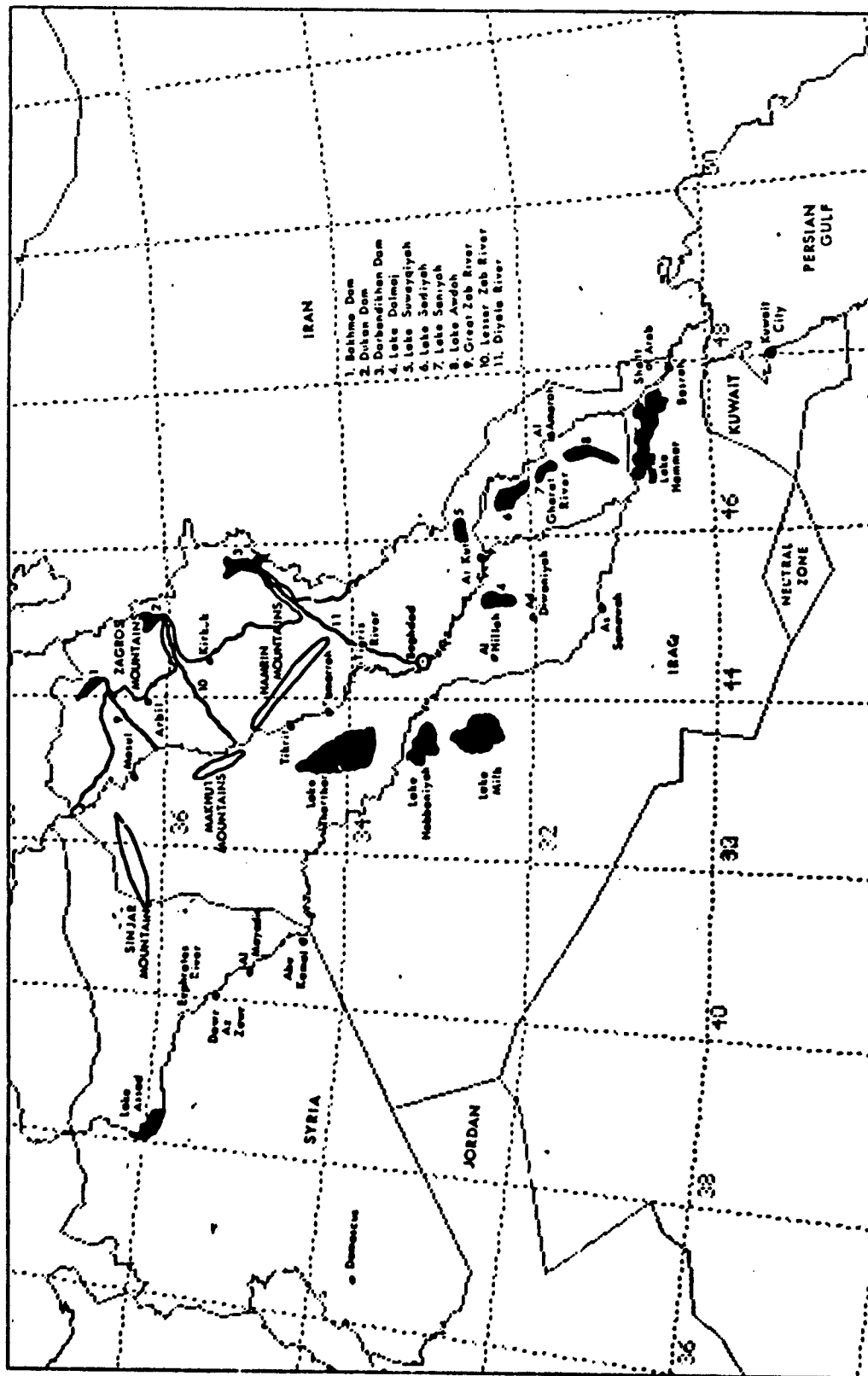


Figure 1-2. Major water features in the area of interest.

2. MAJOR DUSTSTORM TYPES

Although duststorms can take a variety of shapes and forms, there are three main types: *shamal*, *frontal*, and *convective*. The most common type across the Middle East is the shamal. Distinctions between types can be vague; storm types often overlap.

2.1. SHAMAL

The term "shamal" means *north* in Arabic (Middleton, 1986). It refers to the prevailing wind direction from which this type of duststorm is produced. Shamal duststorms occur across Iraq, Kuwait, and the Arabian Peninsula. They generate a tremendous amount of dust in the atmosphere. Shamal systems produce an impressive satellite image and severely reduce visibilities at the surface. A variation of the shamal occurs in the interior of Iran, primarily near the Lut and Margo Deserts. The winds travel across central and southern Iraq, picking up most of their dust load from source areas in the southern portion of Iraq between the Tigris and Euphrates Rivers. There are two types of shamal: summer and winter.

2.1.1 The Summer Shamal

The summer shamal, or "wind of 120 days," blows almost daily during the summer months of June through September. In Kuwait, the shamal is known as the "simoon," which means *poison wind* (Middleton, 1986). The synoptic feature that creates the potential for the shamal is a zone of convergence between the subtropical ridge extending into the northern Arabian Peninsula and Iraq from the Mediterranean Sea and the Monsoon Trough across southern Iran and the Southern Arabian Peninsula.

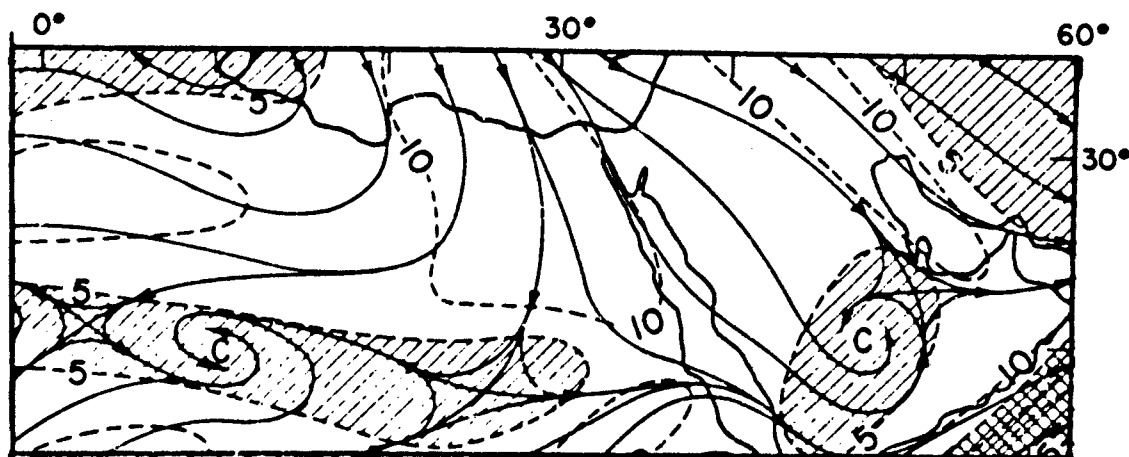


Figure 2-1. Average climatic gradient-level windflow in July (Atkinson, 1971).

As shown in the figure, the pressure pattern tends to be extremely flat across the Arabian Peninsula; a detailed streamline analysis of surface, gradient, and 850-mb levels is generally the best way to detect synoptic features. The zone of convergence between systems is caught between the pressure systems and the Zagros Mountains of western Iran, the orientation of which tends to force an acceleration of the northerly low-level winds across southeastern Iraq, the western Khuzistan Plains of Iran, Kuwait, and the northern Persian Gulf, and into the northeastern Arabian Peninsula.

Although the pressure pattern is favorable for raising dust into the atmosphere, it appears that the influx of cool air aloft (Coles, 1938) adds to the effects of the strong surface heating. This steepens the lapse rate and creates the instability necessary for lifting dust particles and keeping them suspended.

The dry desert air and a high rate of thermal radiation at night forms an inversion between 1,000 and 2,000 feet soon after sunset. The presence of this inversion, along with the pressure pattern, gives rise to a strong wind maximum just above this inversion, known as the "nocturnal jet" (Membery, 1983). The presence of the nocturnal jet has been related to a large number of duststorms across this area; minimum visibility in summer duststorms has been shown to be proportional to the speed of the 1,000-foot wind at Shaibah (located in southern Iraq at 30° 25' N, 47° 35' E to the west of Basrah) at 0500L (Coles, 1938). In more than half the cases, this wind maximum tended to decrease from the nighttime to the daytime sounding.

During the summer, thermal turbulence across the Arabian Peninsula extends above 12,000 feet (Marcal, 1980). The summer shamal takes a characteristic shape from the windflow pattern: as shown in Figure 2-2, it follows a similar life cycle through each episode

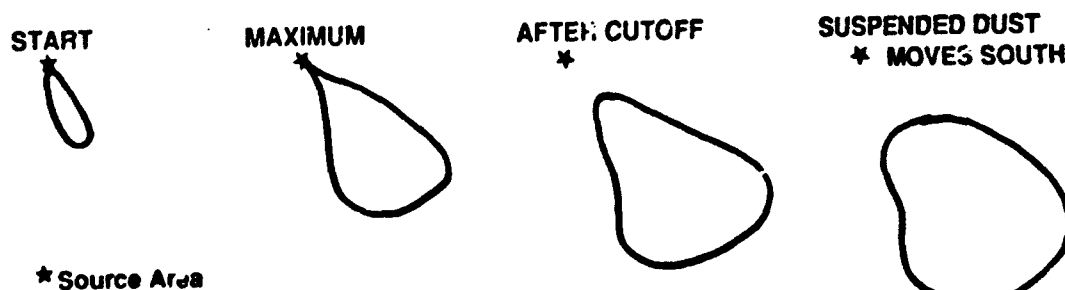


Figure 2-2. Typical dust plume life cycle.

As convergent windflow across central and southeastern Iraq moves over the dust source areas, it lifts dust into a characteristic plume (Kalu, 1979). Within a few hours, the plume stretches southward across Kuwait and the northern Persian Gulf. As the dust enters the northeastern Arabian Peninsula, the windflow becomes divergent; the plume becomes wide on the front edge, tapering back to a point at the source area and taking on a triangular shape. By late afternoon, the winds begin to decrease at the source area; the plume becomes more rounded and does not extend all the way back to the source (see Figures 7-1 through 7-7). Suspended dust in the plume continues to move along with the winds at the gradient level. If there is a cyclonic circulation center in the Monsoon Trough, the dust circulates into it through the night (see Figures 8-1 through 8-3). The dust remains in suspension as long as the upward vertical component in the atmosphere is greater than the minimum required to hold the particles aloft (Gillette, 1979).

Summer shamal duststorms move into an area like a giant wall of dust. The height of the wall averages 3,000-8,000 feet, but in extremely strong storms they can reach 15,000-18,000 feet (Extreme heights are based on satellite derived temperatures of the sand signature as compared to climatic normal temperatures at standard layers of the atmosphere across the Middle East). Visibilities at the surface rapidly go from unrestricted to near zero in a matter of minutes, staying low for 1-3 hours before beginning to increase slowly. As the suspended dust is advected away from the area, visibilities rapidly improve through the night. If the winds aloft have diminished to the point at which the suspended dust is not advected away, visibilities improve slowly to 3 or 4 nm before sunrise, then drop again as sunrise brings increased retraction in the dust and the weakened inversion allows the denser dust to settle.

A simple rule of thumb for the time required for dust particles to settle after the wind has diminished is 1,000 feet per hour. Suspended dust particles have a bimodal size distribution (Hooek, 1984). Smaller particles are only a few microns in diameter, but most range from 20 to 40 microns. Particles capable of traveling long distances usually have diameters of less than 20 microns (Gillette, 1979). The preliminary results of a soil analysis conducted on a Saudi Arabian sample taken just west of Dhahran during DESERT STORM revealed that more than half (56.17%) of the sample was smaller than 250 microns in diameter, and that more than 28% was smaller than 125 microns. The sample content was 60% sand, 40% silt, and 0% clay. Chemical content included quartz (SiO_2), calcite (CaCO_3), and gypsum (CaSO_4) (Henley, 1990). Soil textures, as classified by Hooek, 1984, are as follows:

Clay - less than 0.002 mm (2 microns) in diameter

Silt - 0.002 mm to 0.074 mm (2 to 74 microns) in diameter

Sand - greater than 0.074 mm (74 microns) in diameter

Sand grains are usually assumed to start at about 74 microns in diameter (Hooek, 1984). Sand generally never achieves true suspension; instead, sand grains travel either by saltation (bouncing along the ground) or surface creep (this is how sand dunes move). The differences between sand and dust travel are shown in Figure 2-3.

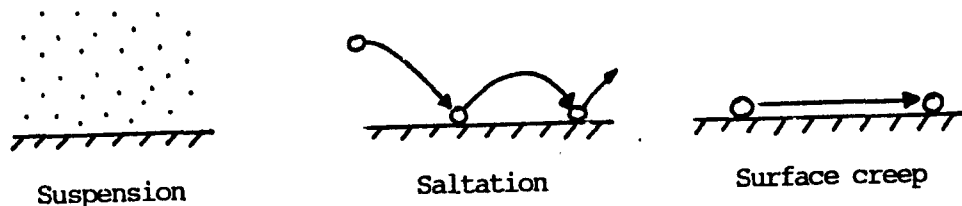


Figure 2-3. How dust and sand travel.

The actual strength of the wind required to lift dust into the atmosphere has been studied extensively. Estimates range from 11 mph/9.6 kts (Bagnold, 1984), to 12 kts (Morales, 1979), and 18 mph/15.6 kts (Coles, 1938). While sand particle movement has been observed at speeds of 8-10 kts, most large scale duststorms require about 15 kts to get started. Winds aloft (at 1,000 feet) need to be about 30 mph/26 kts over Hinaidi, Iraq (Now known as Hindiyah, at 32° 32' N, 44° 14' N, south of Baghdad) (Coles, 1938) and 30 kts over Bahrain (Membrey, 1983). About half of all duststorm occurrences had surface wind speeds of 11-20 kts, while about a quarter had speeds greater than 20 kts (Awad, unkn). Winds average from 15 to 25 kts, with occasional gusts to 30 or 35 kts.

A rough estimate of vertical upward velocity can be obtained by dividing surface windspeed by five; that is, 25 kts of horizontal wind speed would result in about 5 kts of upward vertical motion (Bagnold, 1984). This value is useful in determining the required lift for dust particles of various sizes, as well as the height to which the dust might be carried. Greater windspeeds increase the probability that dust will be lifted and substantially reduce visibilities. Winds, however, must blow over an area susceptible to erosion in order to produce a major duststorm.

Duststorms associated with the summer shamal can have varied durations. They can last just 1 day or from a week to 10 days. Generally, since winds diminish at night, the dust source is cut off. But at Hinaidi, Iraq, most nighttime duststorms are in July and most late evening storms are in May. Most early morning storms at Hinaidi and Shaibah are in June (Coles, 1938).

Since the summer shamal is created by a synoptic-scale pressure system, it usually lasts about 3 days. In late July and August, cyclonic circulations in the Monsoon Trough become evident as dust wraps into these systems and provides a strong satellite signature, particularly in the morning and evening when the sun angle is low and shadows on top of the dust cloud become visible (See Figures 7-6 and 8-1 through 8-3). Figure 2-4 gives mean surface positions of the Monsoon Trough in July and August.

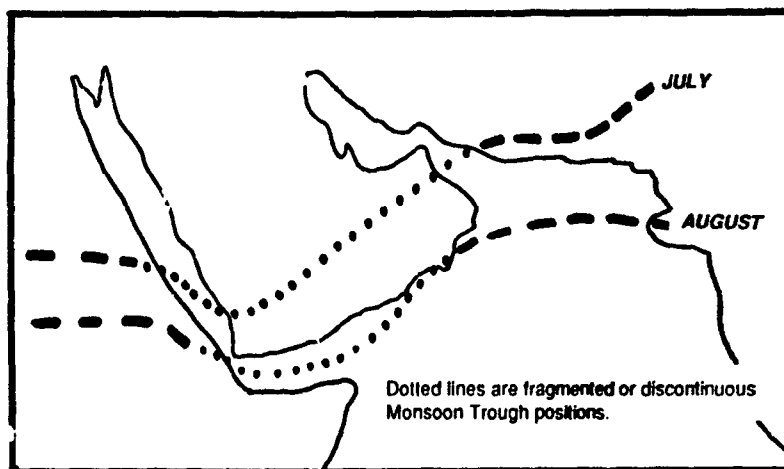


Figure 2-4. Mean surface positions of the Monsoon Trough in July and August. Dotted lines over the Red Sea/Gulf of Aden corridor represent fragmented or discontinuous positions (from USAFETAC/TN--91(X)2).

2.1.2 The Winter Shamal

Figure 2-5 shows mean airflow across the study region in January. A large number of winter shamal duststorms occur as cold frontal systems cross the area; these will be discussed in 2.2. The few winter shamals not associated with frontal systems are created by the funneling of very cold air masses from Turkey or Syria toward the south down the Tigris/Euphrates River Valley in Iraq and over the Persian Gulf. These systems react in the same manner as a fall wind; the air masses are so cold that the fall in elevation does not adiabatically warm them to the surrounding temperature. Fall winds result in a thermal discontinuity and a narrow tongue of cold, dry and gusty winds.

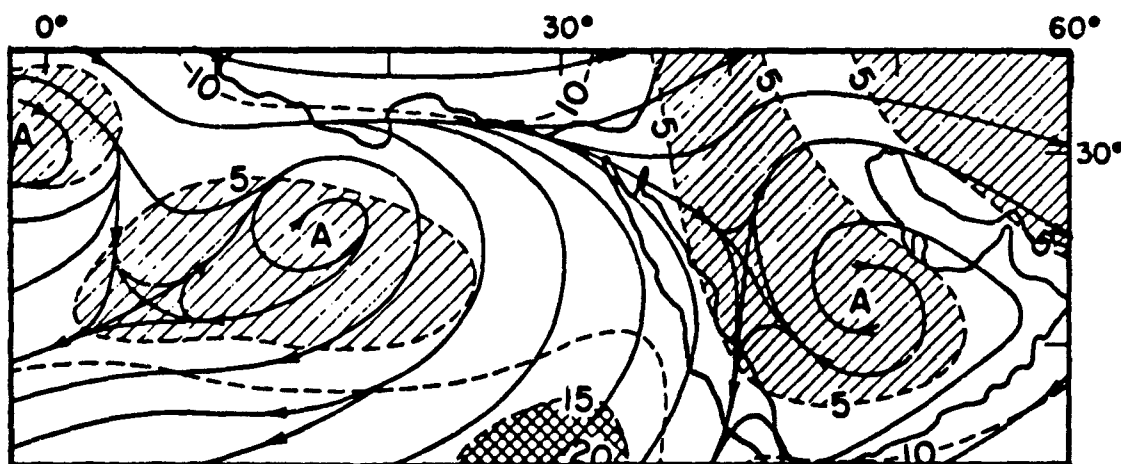


Figure 2-5. Average climatic gradient-level windflow in January (Atkinson, 1971).

The tongue of cold air forms what is called a "density current head" (Lawson, 1971). This river of denser air flows downhill, forcing anything in its path aloft. As a stream of backward-flowing warmer air is forced aloft, dust and debris are lifted (Compton, 1977). See Figure 2-6 for illustrations of both processes. Within the colder air, the movement creates both vertical and horizontal, solenoidal circulations along the leading edge of the gust front; these circulations lift and mix the dust particles. This solenoidal circulation is also found in the horizontal vortex that occurs in thunderstorm downrushes or microbursts (Fujita, 1986). This type of shamal continues until the influx of mass (the cold air) has stopped.

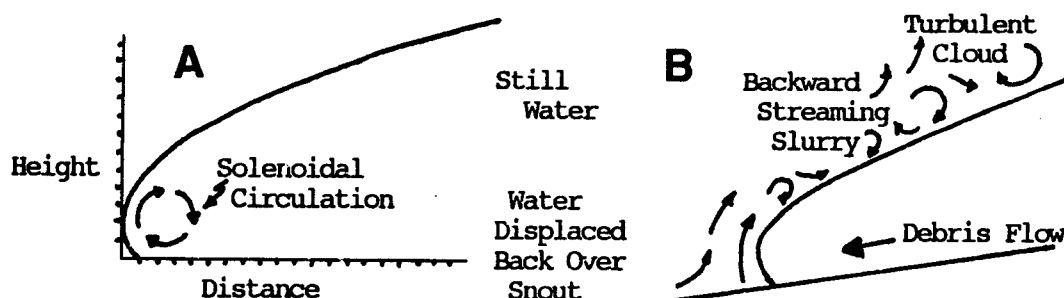


Figure 2-6. Lawson's Density Current (A) and Compton's Turbidity Current (B).

Examples of fall winds include the mistral of the western Mediterranean Sea that occurs around the Gulf of Leon, and the bora of the eastern Mediterranean Sea, which usually extends out of the Black Sea through the Dardanelles and over the Aegean Sea. If the terrain has not been dampened by a preceding frontal system, a duststorm may be generated as these winds pass over source areas.

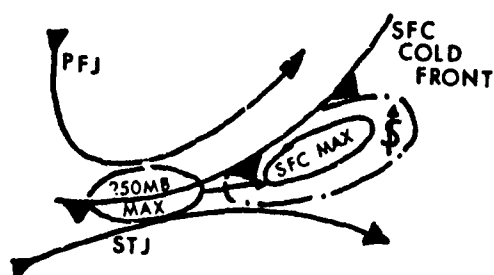
2.2. FRONTAL DUSTSTORMS

The frontal duststorm is on a larger scale than the others. Frontal storms are dynamic synoptic systems that mix the dust in the air and carry it for great distances. The three types of frontal duststorms are *prefrontal*, *postfrontal*, and *shear-line*. Each occurs at a specific time in the life-cycle of a migratory low-pressure area with a frontal system, and each has its own local name.

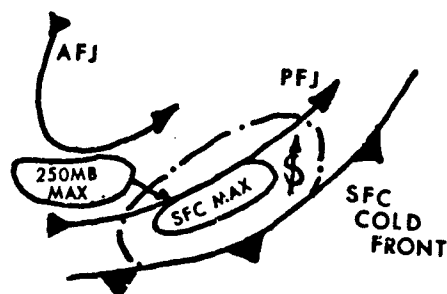
2.2.1 Prefrontal Duststorms

Prefrontal duststorms occur across Jordan, Israel, the northern Arabian Peninsula, Iraq, and the western Khuzistan Plains of Iran as low-pressure areas move across the region. Antecedent factors include a band of winds generated by the low-pressure area that presses against either a stationary high-pressure center in Saudi Arabia or into the western slopes of Iran's Zagros Mountains. The polar jet stream (PJ) behind the front and the subtropical jet stream (STJ) in front of it often converge into a single jet maximum that translates to the surface northeast of the upper-level maximum. In addition, the overlapping of these jet cores and coupling of secondary circulations in the right rear of the PJ and left front of the STJ enhance upper vertical velocities and increase the lifting force for blowing dust.

The two best-known names for these prefrontal winds are the Sharki in Iraq and the Kaus in Saudi Arabia (Middleton, 1986). Others are the Shlour in Syria and Lebanon and the Khamsin in Egypt. Most are southeasterly or southerly, but the Shlour, Kaus, and Khamsin can also be southwesterly. The dry southwesterly Suahili (Soltani, 1990) occurs after the Kaus, which, in extreme cases, can be postfrontal and extend across Jordan, northern Saudi Arabia, Iraq, and Kuwait. At Baghdad, the Sharki and Kaus winds cause more than a third of all instances of blowing dust; easterly to southerly are the favored directions from October to April (Awad, unkn). Figure 2-7 diagrams the prefrontal and postfrontal Kaus wind. For typical Sharki and Kaus satellite imagery signatures, see Figure 2-10A on page 12.



Prefrontal Kaus



Postfrontal Kaus

Figure 2-7. Prefrontal and postfrontal kaus winds diagrammed.

TABLE 1. Percentage frequencies of wind directions during dust disturbances at Baghdad (annual averages), 1950-1960 (Awad).

Quadrant 1	Quadrant 2	Quadrant 3	Quadrant 4
(1-90°)	(91-180°)	(181-270°)	(271-360°)
11.9%	27.7%	7.3%	53.0%

TABLE 2. Percentage frequencies of wind speeds during dust disturbances at Baghdad (annual averages), 1950-1960 (Awad).

0 to 10 kts	11 to 20 kts	More than 20 kts
27.0%	46.4%	26.5%

TABLE 3. Average number of days with duststorms at Baghdad (Awad).

Jan	Feb	Mar	Apr	May	Jun	Jul	Aug	Sep	Oct	Nov	Dec	Total
1.1	2.4	2.5	2.0	1.5	3.3	2.0	1.4	0.7	1.7	1.0	0.9	20.5

TABLE 4. Percentage frequencies of wind directions during dust occurrences at selected stations (annual averages), 1973-1989 (ISMCS, 1990). The map (Figure 2-8) gives locations (by number) of stations in the table.

	Quadrant 1	Quadrant 2	Quadrant 3	Quadrant 4
	(1-90°)	(91-180°)	(181-270°)	(271-360°)
1. Baghdad, IQ	21.8%	31.2%	4.2%	22.8%
2. Mosul, IQ	16.4%	19.5%	33.6%	30.5%
3. Basrah, IQ	14.8%	23.2%	22.2%	39.8%
4. Dayr Az Zawr, SY	18.8%	18.9%	21.3%	41.0%
5. Damascus, SY	15.8%	27.6%	31.1%	25.5%
6. Kuwait City, KW	21.4%	22.6%	19.1%	36.9%
7. Ahwaz, IR	9.1%	20.4%	26.6%	43.9%
8. Dhahran, SD	33.4%	12.9%	12.4%	41.3%
9. Riyadh, SD	25.0%	19.4%	26.6%	29.0%
10. Jeddah, SD	21.0%	31.5%	35.1%	12.4%

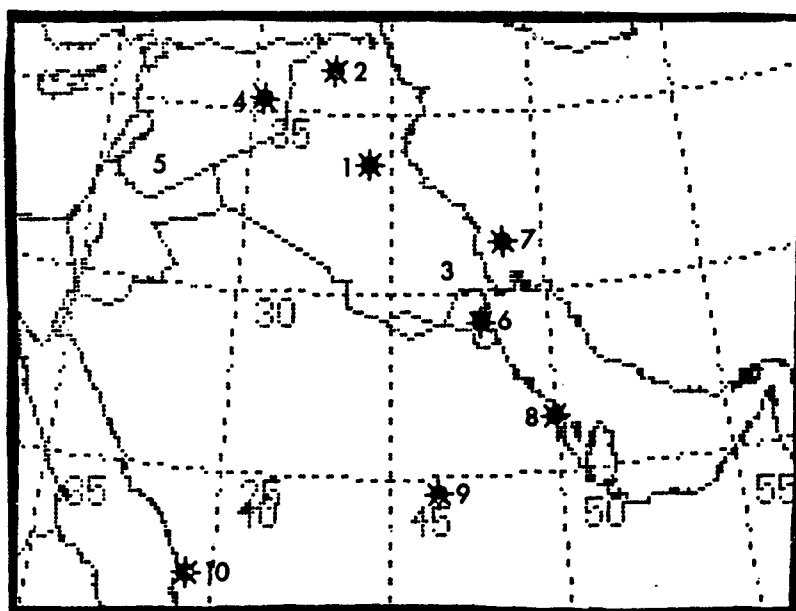


Figure 2-8. Locations of stations corresponding to the numbers in Tables 4 and 5.

Compare the Baghdad statistics in Table 4, which contains more recent climatology statistics for several stations throughout the Middle East, with Tables 1-3. Baghdad's Quadrant 4 wind direction distribution during dust occurrences is not as large, but the peak in Quadrant 2 is still present. The Quadrant 4 change may be due to recent industrial development in that direction.

TABLE 5. Average number of days with blowing/suspended dust/sand at selected stations (ISMCS, 1990). The data in this table includes blowing sand and suspended sand/dust, but not haze. Asterisks (*) indicate less than .5 day. The data from Iran and Iraq was sporadic--none at all was received from 1981 to 1988.

	Jan	Feb	Mar	Apr	May	Jun	Jul	Aug	Sep	Oct	Nov	Dec
1. Baghdad, IQ	6	7	10	14	17	19	20	18	18	17	8	6
2. Mosul, IQ	*	1	3	4	9	12	13	13	8	6	3	2
3. Basrah, IQ	3	4	9	11	10	14	17	14	9	7	5	2
4. Dayr Az Zawr, SY	*	1	2	4	3	7	10	7	3	3	1	1
5. Damascus, SY	1	2	3	5	4	3	2	1	2	3	1	1
6. Kuwait City, KW	9	11	14	15	18	21	19	7	13	12	10	8
7. Ahwaz, IR	*	*	2	3	3	6	4	2	2	1	1	*
8. Dhahran, SD	8	9	11	13	15	21	8	16	9	7	6	6
9. Riyadh, SD	13	14	19	18	19	18	15	3	11	9	11	10
10. Jeddah, SD	7	6	8	7	5	6	5	4	5	2	3	5

Wind speeds associated with prefrontal duststorms are 10-20 kts, with occasional gusts to 25-30 kts; speeds tend to be lower than those of the shamal or postfrontal winds. Across Jordan, particularly near Ma'an (at 30° 12' N, 35° 45' E), winds have been observed to exceed 50 kts in extreme cases associated with the Kaus; these storms may occur once a year and may not recur for several years. Because they are located over similarly shaded terrain on satellite imagery, they are generally more difficult to detect unless they move across the Persian Gulf, the lakes in Iraq, the Red Sea, or the Mediterranean. Frequently, cloud cover associated with an overrunning jet stream obscures the surface features totally.

2.2.2 Postfrontal Duststorms

Postfrontal duststorms are referred to as winter shamals across most of the Middle East, but they have other local names, such as the Blat (Soltani, 1990) or the Belat (Middleton, 1986) in southern Saudi Arabia. These duststorms move in association with a dynamic weather feature and are very active. See Figure 2-10B for a typical satellite signature.

If there is a lot of cloudiness over the surface frontal boundary, the dust signature may be obscured; but in most cases, the dust is the best way of locating the leading edge of the cold frontal airmass. Visual satellite imagery will show a large area of uniform shading as the cloud signature, while infrared imagery will show a dome of dust/sand covering a large part of the Arabian Peninsula. The problem with visual imagery is that unless one is completely familiar with the terrain, the dust may not appear obvious unless it travels over a darker water surface. Since a front is a density current, vortical motions like those shown in density current surges are also generated along the surface frontal zone. These horizontal and vertical vortices (solenoidal circulations) lift and suspend dust and sand particles. They also create the turbulence needed to generate large scale duststorms. Heights of postfrontal duststorms are between 8,000 and 15,000 feet, but dust and reduced visibilities over the American southwest have been reported above 30,000 ft by USAF pilots debriefed at Holloman AFB, New Mexico.

Zero visibilities are not uncommon in postfrontal storms. Surface winds are 15-30 kts, but gusts can be over 40-50 kts in stronger systems. According to Peer (1984), intensity of a winter shamal outbreak can be determined using thermal contrast across Iraq. A contrast of 10° C equates to 30 kts, 15° C to 35 kts, 20° C to 40 kts, and 25° C to 45 kts. Gust speeds will be 10 kts higher than sustained winds: peak gusts will be up to 20 kts higher.

There are two types of winter shamal. The first lasts for 24-36 hours as a frontal system migrates through the region; the shamal winds and blowing/suspended dust move across the length of the Persian Gulf in 12-24 hours and can be along the southern coast of the Arabian Peninsula and Iran within 48-72 hours (see Figures 6-1 and 6-2). The second type persists for 3-5 days when a front stalls out and becomes stationary (Perrone, 1979). Frequently, the longer shamal has cyclogenesis occurring along the frontal boundary with a parallel jet stream moving the frontal waves to the east-northeast.

2.2.3 Shear-line Duststorms

The final type of duststorm associated with frontal systems is the shear-line type--See Figure 2-9 for Atkinson's model of a surface shear line and Figure 2-10C for a typical shear line duststorm satellite signature. Shear lines are frequent in winter across the Arabian Peninsula, the Red Sea, and throughout equatorial Africa.

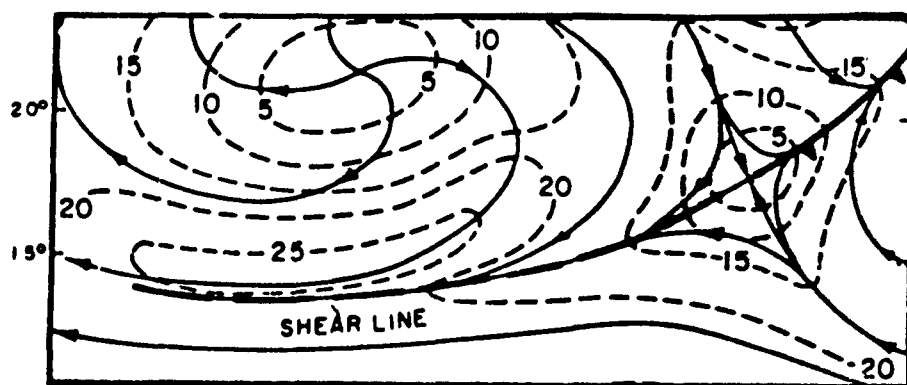


Figure 2-9. Atkinson's model of a surface shear line. The diagram includes streamlines and isotachs over a tropical area.

Shear lines are created by convergence of northeasterly windflow to the south of a polar high-pressure cell and the easterly trade-wind flow. Along the shear line there is a narrow band of maximum winds that lifts loose dust particles into the air as the shear line moves slowly southward and extends back to the west. Visual satellite imagery shows some traces of the dust as opaque white; infrared imagery will show plumes of dust in the cold air side and along the shear line. A frequent sight across north Africa is dust funneling through and between mountains, leaving a rainshadow-type image (see Figure 6-6). A common sight in visual imagery is that of dust advecting off the western coast of Africa. The same shear-line pattern occurs over the Arabian Sea as the cold front weakens across Pakistan or northwestern India and leaves a shear line across the sea. The addition of moisture here will also create a narrow band of rope clouds along the convergent frontal zone, with blowing dust to the northern side of the cloud (see Figure 6-2).

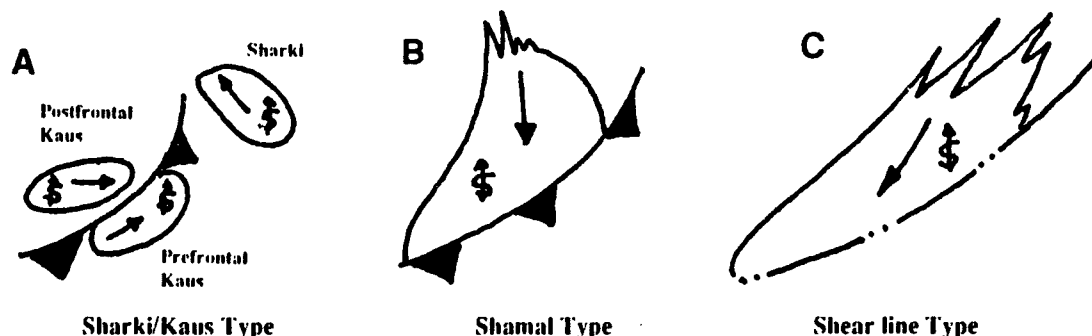


Figure 2-10. Comparisons of signatures in satellite imagery.

Wind speeds along a shear line are usually 10-25 kts with gusts of 30-40 kts. Across north Africa, the shear line and associated duststorms become almost semipermanent features. They become temporarily stronger if the ridge moves southward or builds, or if it is reinforced by frontal intrusions from the north. The climatological pattern across central Africa has converging winds between the high pressure to the north and the tropical easterlies to the south. Blowing dust generally does not occur with this pattern, primarily because there isn't enough lift. Temperature contrast, along with temperatures lower than normal and pressures higher than normal are good indications of shear line existence. There are many similarities with the traveling microburst (Fujita, 1986) and wind maxima that can be tracked to the west along the shear line: the microburst, however, is shown with divergent flow and decreasing winds, whereas the shear line has converging winds. These maxima are accompanied by duststorms and low visibilities as they move over sources of loose surface material. Visibilities can fall to less than 1/2 nm, but are usually in the 1-3 nm range.

2.3 CONVECTIVE DUSTSTORMS

These features are normally of a much smaller scale than frontal or shear-line storms, and therefore more difficult to forecast. Their effects on desert operations, however, are still significant. There are two types of convective duststorm: The *haboob* and the *dust devil*. The *haboob* has received considerable attention in the past 10 years, primarily due to its involvement in the failed Iranian hostage rescue attempt of 1980 (Ryan, 1985), as well as several aircraft crashes related to microbursts (Fujita, 1986), one of the features that generate *haboobs*.

2.3.1 The *haboob*

The *haboob* is a duststorm generated by downrush winds from a thunderstorm. It gets its name from its frequent occurrence over the deserts of northern Africa, but it also occurs and has been studied in the American southwest (Idso et al, 1972).

As cool sinking air and heavy rains bubble out from under a thunderstorm, a zone of stronger winds and a mesoscale high-pressure area is created. In the desert, the surrounding air is so dry that most or all of the rain evaporates before reaching the ground. The wind, however, continues. It blasts into the dry desert surface, picking up large amounts of loose dust and sand (see Figure 9-1). The dome of cool air thus created has been likened to the density current (Compton, 1977) mentioned earlier in the discussion of the shamal. There are small solenoidal circulations (called the "horizontal vortex" by Fujita) within the cool air--see Figure 2-11. Along the leading edge of the haboob, rapidly rising and changing towers and buttresses can be seen (Powell, 1969). Combined with the warm air being forced aloft, the primary ingredient for a vigorous duststorm is generated.

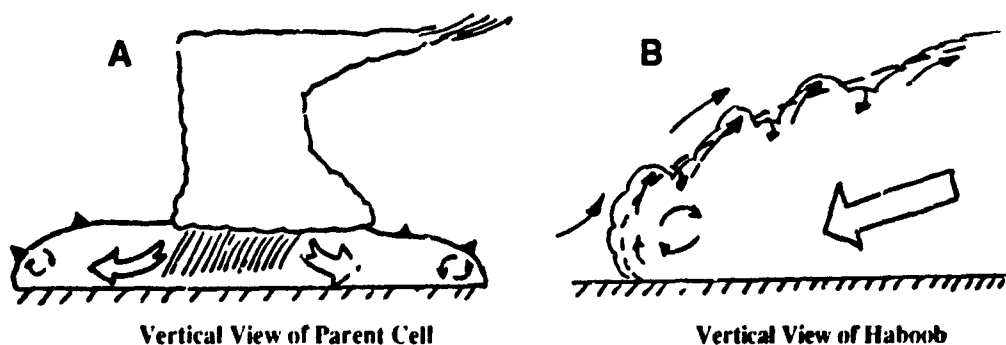


Figure 2-11. The formation of a haboob. In A, solenoidal circulations in the downrush are shown. In B, the haboob is developing at the leading edge of the downrush.

Although relatively small (they usually cover no more than 60-90 miles), haboobs can be violent, with damaging winds. In Phoenix, AZ, the average haboob wind is 48 mph (42 kts), but the maximum reported speed was 72 mph (63 kts) (Idso et al, 1972).

Although they can be seen approaching the station from afar, haboobs move in very quickly. The average height of these storms ranges from 5,000 to 8,000 feet, but they have been known to reach 10,000-14,000 feet (Idso, 1976). As the cool air mass of the storm passes over a station, the temperature falls within the first 50 meters. Although the change may be just a degree or two ($^{\circ}\text{C}$), the average in Phoenix is 7°C (Idso et al, 1972). Visibilities in the storm also fall rapidly to 200 meters (1/8 nm) or less inside the haboob (Lawson, 1971). Visibility usually increases within an hour; average duration is 3 hours, but the maximum is 5 1/2 hours (Idso et al, 1972).

Peak wind speeds in the haboob are usually 95% greater than the speed of movement (Lawson, 1971); that is, if the haboob approaches at 25 kts, the maximum wind inside would be 48 kts.

Haboobs are the true walls of dust and sand that most people think of as a strong duststorm. Most dust particles within these storms are from 10 to 50 microns (Lawson, 1971), but larger particles (up to several millimeters) can and will be blown about (Foster, 1969). The larger particles settle rapidly after the wind subsides, but the finer ones settle at about 1,000 ft per hour where the haboob finally dissipates. Other areas clear rapidly as the dust is advected out of the area.

2.3.2 Dust Devils

These are small cyclonic circulations that form in arid climates when there is an extremely steep lapse rate with strong surface heating. Dust devils pick up dust and sand, or anything else loose, but they are generally visible and easy to avoid as they occur sporadically across the desert. They range from a few feet in height and diameter to several hundred feet in diameter and heights of 3,000-6,000 feet. Winds in dust devils at Holloman AFB, NM, have been measured at 48 kts--see Figure 2-12 for a typical dust devil wind recorder trace.

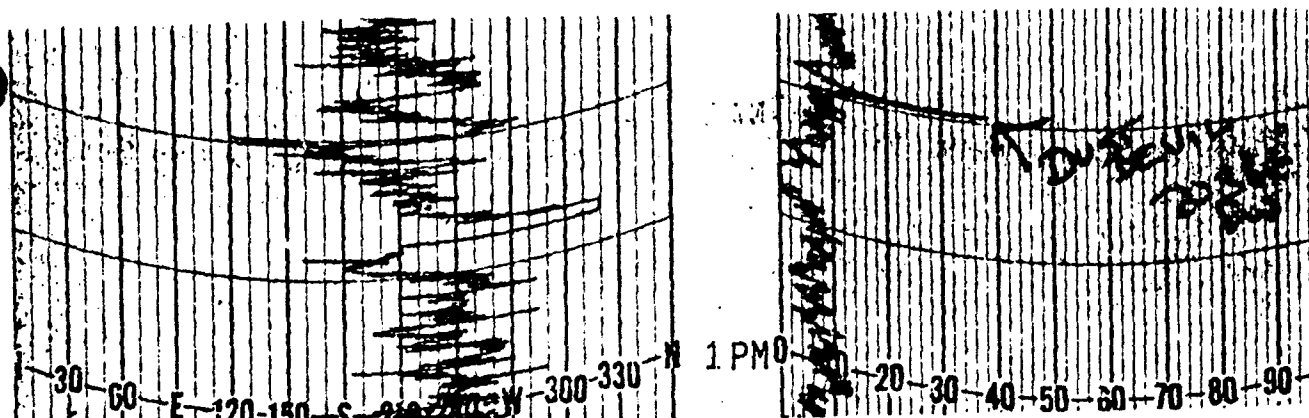


Figure 2-12. Wind recorder trace of dust devil at Holloman AFB, NM, 22 April 1976.

Some tools used for forecasting dust devils in the American southwest may be useful elsewhere. Surface conditions must be dry for at least 2 or 3 days with no precipitation. April is normally the first month of occurrence in the southwest, when temperatures reach to about 80° F. A weak gradient, with light and variable winds, is most favorable. Skies are usually clear or scattered with high clouds. When dust devils form with light (less than 5-kt) winds, they move toward higher terrain over ground with slight slope. Settling rate is assumed to be 1,000 ft per hour, but dissipation leaves little trace of most dust devils.

3. DUSTSTORM SOURCE REGIONS

Most deserts are not the continuous expanses of sand we normally picture when we think of northern Africa and the Sahara. The Sahara is, in fact, a sea of sand in some areas, but most deserts actually have an abundance of life that ranges from various plant forms to a number of animals that have adapted to survive. Desert surfaces vary from fine dust to a more common pebble surface with patches of sparse plant life, usually sage brush, cactus, hardy grass, or small trees. Each of these plant forms has several functions. One is to provide food and shelter to desert animals, and another is to keep the desert surface intact.

Uncovered soil is easily weathered or eroded by wind, whereas vegetation makes erosion more difficult. Plant cover provides a root complex that holds the soil together and raises the zone of friction between the ground and the overlying winds. Plants slow the winds by increasing friction and keep the wind from picking up dry soil. In areas of vegetation, blowing dust usually only occurs with strong winds produced by strong synoptic features, or after a long dry period. Note that blowing dust is produced when a thin layer of the surface is loosened or disturbed, usually by animal or vehicle traffic.

Some areas are more susceptible to erosion than others; they are therefore better source areas. Improper irrigation over long periods leaves poor soil with a high saline content due to high evaporation rates. In infertile dry lakebeds, evaporation often leaves a fine crust of salt on the surface. In dry river beds, the occasional seasonal wash keeps the vegetation small; surface material is sorted by size and relatively loose. Desert areas are also sources for large quantities of gypsum, usually left by ancient water bodies. Underground salt domes are usually present in oil-rich areas where plant growth is discouraged. All these areas are prime sources for sandstorms when wind speeds reach the speeds necessary to lift dust off the surface.

3.1 MESOPOTAMIAN REGION DUSTSTORM SOURCES

The Mesopotamian source region includes Syria, Iraq, western Iran, and the northeastern Arabian Peninsula. Individual duststorm source areas in this region, numbered 1 through 14, are described in turn. All have a west to north wind component. Large-scale pressure systems such as fronts are not discussed because such systems carry widespread dust along with them and prevent detection of the actual source areas. Figure 3-1 is a template map of the Mesopotamian region, drawn from an ascending DMSP satellite imagery scale; it can be reproduced as a transparency and used to locate each of the numbered source areas for forecasting purposes.



Figure 3-1. Mesopotamian template map. DMSP F-7 imagery from 24/0607Z October 1984.

Mesopotamian Source Area 1 lies east of the ruins of Babylon ($32^{\circ} 33' \text{ N}$, $44^{\circ} 25' \text{ E}$) at Hilla Iraq ($32^{\circ} 28' \text{ N}$, $44^{\circ} 29' \text{ E}$), and to the west of Hawr (Lake) Dalmaj ($32^{\circ} 20' \text{ N}$, $45^{\circ} 30' \text{ E}$). It is in the center of the alluvial plains of the Tigris/Euphrates Rivers. It tends to be marshy in the wet seasons. In satellite imagery, the area looks slightly higher and lighter than the surrounding terrain. The duststorm track has been observed to run from as far east as Abadan, Iran ($30^{\circ} 20' \text{ N}$, $48^{\circ} 15' \text{ E}$) to as far west as western Kuwait, but the usual track is across Basrah, Iraq ($30^{\circ} 30' \text{ N}$, $47^{\circ} 50' \text{ E}$) and over eastern Kuwait. The period of observed duststorm activity is from May to October--winters and springs tend to be too damp.

Mesopotamian Source Area 2 lies in the alluvial plains between the Tigris/Euphrates Rivers; it is to the south of Ad Diwaniyah, Iraq ($32^{\circ} 00' \text{ N}$, $44^{\circ} 57' \text{ E}$) and northwest of Samawah, Iraq ($31^{\circ} 18' \text{ N}$, $45^{\circ} 18' \text{ E}$). Duststorm activity is restricted mainly to summer and fall; the area is damp and surrounded by marshes the rest of the year. In satellite imagery, the area looks higher and lighter than surrounding terrain. The duststorm track ranges as far east as Basrah, Iraq, and as far west as western Kuwait and the Neutral Zone, but the usual track is over Kuwait.

Mesopotamian Source Area 3 lies east of El Rashid (Raqqa), Iraq ($35^{\circ} 56' \text{ N}$, $39^{\circ} 02' \text{ E}$) to the north of the Euphrates River and south of the Abdul al Aziz Mountains. No seasonal restrictions have been observed, but most activity is in summer. Again, this area looks lighter in satellite imagery, and appears to be highlands just north of the Euphrates River valley. The duststorm track normally extends to the east or southeast into northwestern Iraq and the al Jazira desert highlands, but dust has been observed extending east to the north of Baghdad ($33^{\circ} 20' \text{ N}$, $44^{\circ} 26' \text{ E}$), then southeast over Ilam ($33^{\circ} 37' \text{ N}$, $46^{\circ} 27' \text{ E}$), and Mehran, Iran ($33^{\circ} 07' \text{ N}$, $46^{\circ} 10' \text{ E}$), and finally south over the Khuzistan plains in southwestern Iran.

Mesopotamian Source Area 4 is to the south of Kut, Iraq ($32^{\circ} 30' \text{ N}$, $45^{\circ} 51' \text{ E}$) between Hawr Dalmaj and Hawr Sa'diyah ($32^{\circ} 25' \text{ N}$, $46^{\circ} 40' \text{ E}$) and Hawr Saniyah ($31^{\circ} 45' \text{ N}$, $47^{\circ} 35' \text{ E}$). Area 4 is in the marshy lowlands of the Tigris River; activity is restricted to summer and fall. The general duststorm track is between Basrah, Iraq, and Abadan, Iran.

Mesopotamian Source Area 5 is to the south of Mehran, Iran, in the Pusht-i-kuh (mountains) area. No seasonal limits have been observed. The general track is to the south over Khuzistan, Iran. In some cases, this area is an extension of duststorms from areas 3 and 9.

Mesopotamian Source Area 6. Duststorms originate from south of Samawah, Iraq, and usually extend over either Kuwait or the Neutral Zone. Although located to the south of the Euphrates River, it is not known whether or not this area remains active through a wet season; satellite imagery suggests that it does not.

Mesopotamian Source Area 7. This relatively weak area lies to the west-southwest of Abu Kamal, Syria ($34^{\circ} 29' \text{ N}$, $40^{\circ} 56' \text{ E}$). Little else is known except that there are summer occurrences of duststorm activity from this area.

Mesopotamian Source Area 8 is to the east of Baghdad, Iraq, and east of the Tigris River. It appears to be an extension of an extreme case from Area 3. It is not known whether or not it lies in the alluvial plains and is subject to seasonal wet periods.

Mesopotamian Source Area 9 is to the southeast of Dawr az Zawr, Syria ($35^{\circ} 21' \text{ N}$, $40^{\circ} 09' \text{ E}$), and east of al Mayadin, Syria. It extends from the eastern Syria desert into the western al Jazira desert highlands; the existence of a seasonal wet period is doubtful. The general duststorm track is eastward to Tikrit, Iraq ($34^{\circ} 36' \text{ N}$, $43^{\circ} 42' \text{ E}$).

Mesopotamian Source Area 10 is to the west of An Nasiriya, Iraq ($31^{\circ} 04' \text{ N}$, $46^{\circ} 17' \text{ E}$) and south of the Euphrates River. The general duststorm track is to the south over Kuwait. It is thought that there is no seasonal wet period.

Mesopotamian Source Area 11 may be an extension of Area 4, but it lies farther south of Kut, Iraq--almost as far south as Refa'i, Jordan ($32^{\circ} 19' \text{ N}$, $36^{\circ} 46' \text{ E}$), or Shatra, Iraq ($31^{\circ} 26' \text{ N}$, $46^{\circ} 10' \text{ E}$) and just to the north of

Hawr al Hammar (Lake Hammar). Satellite imagery shows it to be lighter in color and apparently higher than surrounding terrain. The duststorm track is to the south over Basrah, Iraq, and Abadan, Iran.

Mesopotamian Source Area 12 ($35^{\circ} 24' \text{ N}$, $38^{\circ} 24' \text{ E}$) lies to the south of Bahrat (Lake) Assad, Syria ($35^{\circ} 50' \text{ N}$, $38^{\circ} 40' \text{ E}$) and north of Tadmur, Syria ($34^{\circ} 36' \text{ N}$, $38^{\circ} 15' \text{ E}$). The duststorm track is east across Dawr az Zawr, Syria ($35^{\circ} 21' \text{ N}$, $40^{\circ} 09' \text{ E}$).

Mesopotamian Source Area 13 is to the south of Dezful, Iran ($32^{\circ} 23' \text{ N}$, $48^{\circ} 28' \text{ E}$). The dust track is south, over the northeastern Persian Gulf.

Mesopotamian Source Area 14 lies to the east-northeast of Ar Ruthah, Iraq ($33^{\circ} 03' \text{ N}$, $40^{\circ} 18' \text{ E}$) near $33^{\circ} 18' \text{ N}$, $41^{\circ} 30' \text{ E}$. The area, which consists of dry lakebeds and streambeds, has been observed in summer and fall; winds range from northwest in the summer to southwest in the fall. It takes a strong surge of winds, usually postfrontal jet convergence, to generate duststorms here.

3.2 SOUTHWEST ASIA DUSTSTORM SOURCES

Southwest Asia includes eastern Iran, Pakistan, Afghanistan, northwestern India, and the south-central USSR. The template map in Figure 3-2 can be used to make overlay transparencies for DMSP ascending node normal grid.

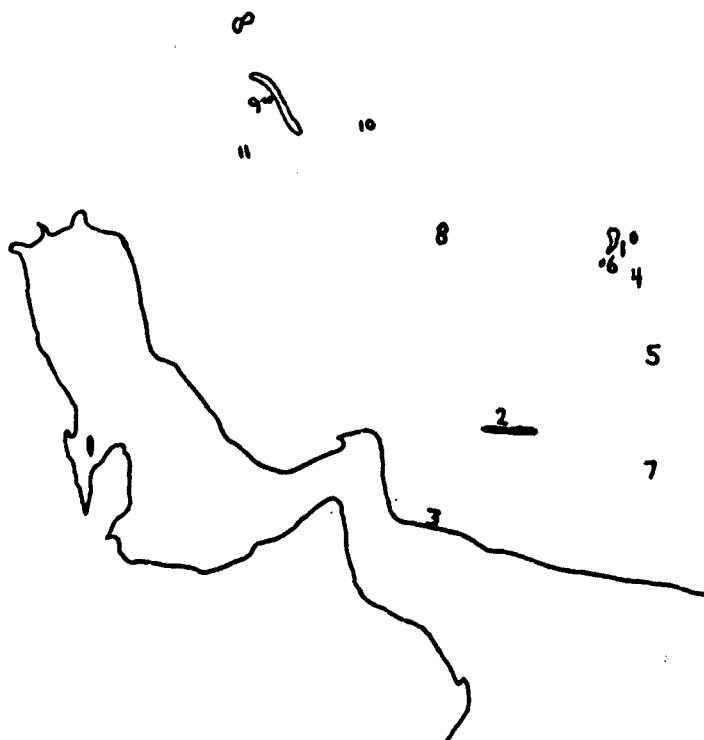


Figure 3-2. Southwest Asia template map. DMSP F-6 imagery from 24/0230Z May 1985.

Southwest Asia Source Area 1 (31.3° N, 61.4° E) lies on the eastern shores of Hamun-e Saberi in eastern Iran and western Afghanistan, just north of Zabol, Iran, and northwest of Zarani, Afghanistan. It is only observed when winds are northwest to north.

Southwest Asia Source Area 2 (27.5° N, 58° E to 27.2° N, 61° E) is a flat area with most sand coming from Hamun-e Jaz Murian, a dry lake bed about .5 degree in diameter at 27.5° N, 58.8° E. Storms usually occur when northwest to north winds push dust southeast to southwest across the Gulf of Oman to the Strait of Hormuz. The three small villages of Zeh Kalat, Surgabad, and Gol Murti are nearby. Since this source region is on an interior plateau in the southern Zagros Mountains, storms are contained by the mountains except in extreme cases.

Southwest Asia Source Area 3 is on the southern Iranian coast of the western Gulf of Oman from 27° N, 57° E to 25.5° N, 60° E. Although it is relatively small, its trajectory takes dust into the Gulf of Oman where it presents a hazard to shipping.

Southwest Asia Source Area 4 is immediately adjacent to Area 1 in western Afghanistan (30.7° N, 62° E) and requires the same northwest to north winds for activation. The area is north of the towns of Karudi, Chahar Borjak and Ashkinak, all in Afghanistan. It is very large and generates massive amounts of blowing dust. Dust from Area 4 moves to the southeast and south and is funneled through a large unnamed pass at 29.2° N, 63.1° E from Afghanistan into Pakistan.

Southwest Asia Source Area 5 is an extension of Areas 1 and 4, but it can generate blowing dust by itself as winds funnel from the north through the pass at 29.2° N, 63.1° E from Afghanistan into Pakistan and southeast to south into the northern Arabian Sea. Area 5 extends from the pass to a dry lake bed at 28.3° N, 63° E. It is .5 degrees in diameter. Although the strongest winds occur after winter frontal passages, summer winds are also strong enough to raise dust.

Southwest Asia Source Area 6 lies to the south of Hamun-e Saberi and northeast of Daryacheh-ye Hamun, northwest of Zabol, Iran. This very small source area needs a northwest to north wind to lift dust.

Southwest Asia Source Area 7 is another dry lake bed, located at 26.8° N, 63.7° E, just west of the town of Panjgur, Pakistan. Mountains offer some protection but winds are strong enough to lift the dust as it blows from Areas 1, 4, and 5 toward the northern Arabian Sea. A gradual decrease in elevation toward sea level enhances dust suspension.

Southwest Asia Source Area 8 is the Dasht-i-Lut (or Kavir-e Lut, the Lut Desert), located at 30.5° N, 59.2° E. There is a dry lake bed along the southern extreme at 29.5° N, 59.1° E. The nearest villages (.5-1.0 degrees south-southwest) are Bam, Allahabad, Fahraj, and Qaleh-ye Chasmeh, all in Iran. Northwest to northeast winds lift the dust and move it southeast to south where it joins with Area 2.

Southwest Asia Source Area 9 comprises a row of dry lake beds that extend from 32.7° N, 53.9° E to 33.8° N, 52.4° E along the eastern slopes of the Zagros Mountains. The nearby villages of Kashan and Ardestan are south of the northern portion, and Na'in is west of the southern portion. This area is sheltered and requires an extremely strong frontal system to generate the strong WSW to WNW winds needed to move the dust.

Southwest Asia Source Area 10 is an extension of Area 9, located at 33.1° N, 55.3° E near Baiazeh. It is also a dry lake bed and it requires the same wind forces as Area 9.

Southwest Asia Source Area 11 is composed of several dry lake beds that lie to the east and southeast of Esfahan at 32.2° N, 53.0° E to 32.4° N, 52.4° E. This is another extension of Area 9, and requires the same strong winds.

3.3 RED SEA AREA DUSTSTORM SOURCES

The Red Sea area includes Egypt, northeastern Sudan, the Sinai, Jordan, and the northwestern half of Saudi Arabia. Figure 3-3 is a template map for clear transparency reproduction and overlay for DMSP ascending node grid.

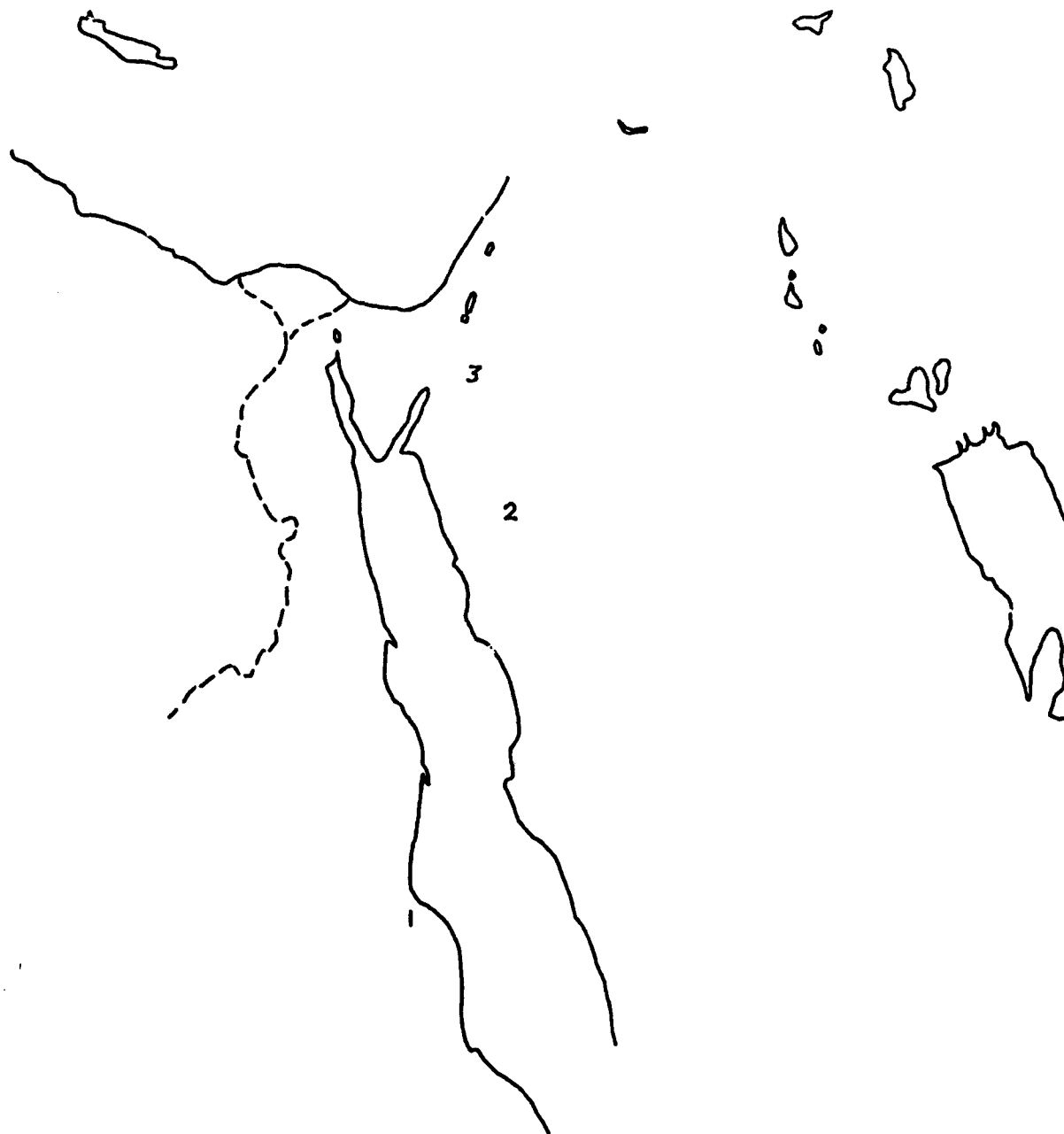


Figure 3-3. Red Sea Area template map. DMSP F-7 imagery from 18/0714Z June 1985.

Red Sea Source Area 1 is at the Tokar Gap (18.2° N, 37.5° E) in northeastern Sudan. Seasonal gradients are responsible for the direction in which the dust/sand is blown. In the summer, the direction is to the northeast and into the Red Sea. Dust frequently blows into the Red Sea for several days, filling the atmosphere from the Tokar Gap south to the Gulf of Aden with suspended dust/haze. In the summer, if thermal low pressure is to the west, dust also blows *into* these cyclonic circulations. During the winter, the dust primarily blows to the west across Sudan because of the stronger high pressure to the northwest. Thermal contrasts and funneling through the Gap tends to intensify the winds; although there are no local weather observations, the sharpness of the dust plume and speed of movement suggest that 30-50 knot winds may be common.

Red Sea Source Area 2 is in the northwestern highlands of Saudi Arabia north and south of Medina. Directions of movement may be as variable as during the summer. After frontal passage, dust tends to travel to the southeast or south. Prefrontal dust (and in extreme cases, postfrontal dust) tends to be blown to the northeast or east. Shear-line dust is confined in the highlands, but on isolated occasions when high pressure builds in northern Saudi Arabia, it is blown west into the northeastern Red Sea.

Red Sea Source Area 3 is a dry lake bed in southern Jordan to the east of Ma'an at 30.3° N, 36.3° E. This is generally a postfrontal area that blows to the northeast and east as frontal convergence moves through. Strong winds (30-40 knots) can occur; winds over the highlands along the eastern Jordan valley usually show evidence of turbulence through the existence of roll and rotor clouds.

4. DUST FORECASTING

Because most blowing sand and dust occurs over the open desert where there are few, if any, weather reporting stations, forecasting these phenomena is extremely difficult. Satellite imagery is clearly the best way to supplement what few observations there are, but accurate forecasting, even with satellite photos, remains a problem. To forecast the onset of lifted dust/sand, a lifting threshold must be established and considered. Once dust is suspended, a settling threshold helps determine the duration of the event. In order to be able to use either of these thresholds, forecasters must have some knowledge of sand/dust particle size in the area of interest. Years of observation and experience with these three elements have yielded some rules of thumb that work in most cases.

4.1 LIFTING THRESHOLDS

Before dust can be lifted, certain atmospheric criteria must be met (Kalu, 1979). Although wind is an important factor, it is not the only one. Obviously, if dust is to be lifted, the ground must be dry enough. Next, there must be upward vertical motion, either by the convection common to deserts, or by a synoptic feature (such as a frontal slope). Finally, since laminar windflow alone will not lift dust, some sort of turbulence must be present to scour the particles away from the desert surface. Once these conditions have been met, all that remains is for wind speed to increase above the lifting threshold established for the dust particles in a particular area.

Lifting threshold is the speed at which the wind is capable of lifting dust particles of a given size into the atmosphere. The actual force required is not only the horizontal wind speed, but the upward vertical speed, as well. Upward vertical speed can be calculated by taking one-fifth of the surface wind speed (Bagnold, 1984). The amount of upward speed required depends totally on particle size; the larger the particle, the greater the upward speed required to keep it aloft. Studies show that upward speeds as low as 1.3 mps (4.3 fps) are capable of keeping 150-micron particles suspended.

Most studies conclude that horizontal thresholds begin at 11-18 MPH (9.6-15.6 kts). One of the best of these studies is documented in Natick Laboratories' Technical Report ES-8, which states that the first particles of dust and sand to move with windspeeds of 11-30 MPH (9.6-26 kts) are those from .08 to 1 mm (80-100 microns) in diameter. Larger particles (1-2 mm) are lifted at 35-45 MPH (36.4-41.1 kts). Particles larger than 2 mm require winds greater than 50 MPH (43.5 kts), and particles larger than 4 mm are seldom moved at all. Particles smaller than .08 mm require sharply higher wind speeds to be lifted. For example, a study conducted in the California desert showed that .002-mm (2-micron) particles were not moved, even by winds greater than 50 MPH (43.5 kts). It would appear, then, that the most common particle sizes (about 1 to 50 microns) have lifting thresholds greater than 11 MPH/9.6 kts (Stewart et al, 1985). Either this breakdown is not completely correct, or the saltation of the first particles to be lifted would cause the smaller particles to be hurled aloft by their impact upon the ground. This tends to be the most likely explanation.

The California study gave a rough list of windspeeds required to lift dust from several different desert environments. The areas known as "playas" in the United States are called "sabkhas" in the Middle East (Walker, 1986). Traffic, whether by people, animals, or vehicles, lowers pickup speeds.

Fine to medium sand in dune covered areas	10-15 MPH (8.7-13 kts)
Sandy areas, poorly developed desert pavement	20 MPH (17.4 kts)
Fine material, desert flats	20-25 MPH (17.4-21.7 kts)
Alluvial fans, crusted playas	30-35 MPH (26.1-30.4 kts)
Well developed desert pavements	40 MPH (36.8 kts)

According to Gillette (1979), dust particles capable of traveling great distances are usually smaller than 20 microns. Since particles associated with most Middle East winds travel the length of the Arabian Peninsula, at least some of the dust cloud must be composed of particles of this size. The larger particles would settle out of the atmosphere (Berkofsky, 1982) close to the source region.

4.2 SETTLING THRESHOLDS

The converse of upward vertical speed (the speed required to keep particles suspended) is "settling speed." Dust remains suspended in the atmosphere as long as there is enough upward vertical motion to keep it there. The speed at which a given particle falls through the atmosphere is referred to as the "terminal velocity" of that particle, a constant (Stewart et al, 1985). As long as the upward speed is greater than a particle's terminal velocity, the particle will remain aloft. Acceleration continues only until the particle reaches its terminal velocity; from that point on, the particle falls at a constant rate so long as no other factors influence it. (Bagnold, 1984).

The terminal velocity of a particle is directly proportional to its size; Gravity acts on the particle in accelerating it downwards, and atmospheric resistance acts against it as it falls. The larger the particle, the faster it descends. For example, studies show that particles descend at the following rates in feet per second (fps): 150 microns at 3 fps, 40-74 microns at 1 fps, and 5 microns at 0.01 fps (Greveris, 1977). Other studies confirm these descent rates; Hooch (1984) found that particles larger than 100 microns fall out at speeds higher than 2.5 fps.

Using Stoke's Law, Lawson (1971) found that particles of between 10 and 50 microns fall at about 1,000 feet per hour (fph), a figure that seems to correlate well with most actual cases. It has been used to determine the lifespan of larger dust devils in the desert southwest of the United States with some success, and has also been used to compute the settling of suspended dust in New Mexico after large-scale duststorms.

Using 1,000 fph, if dust is lifted to 5,000 feet and the wind drops to below terminal velocity (assume it to be light and variable), the dust will settle in about 5 hours. Settling is by particle size, with the largest falling out first and the smallest falling out last. The fallout occurs over a distance if the dust cloud is advected, with the larger and heavier particles settling near the source area and the smaller ones settling some distance away. Examples can be seen across the Arabian Peninsula, where smaller particles have settled for years in the southern portion now known as the "Empty Quarter," a vast sea of sand.

4.3 EFFECTS OF PARTICLE SIZES

Particle size plays an important part in both lifting and settling thresholds. It is not a simple case of the smallest particles being lifted first with weak winds, however. The fact is that a favored size is lifted first, followed by an apparent bell-curve effect with gradually increasing windspeeds. Settling, on the other hand, is based strictly on the effects of gravity and atmospheric resistance. Longer suspension times for smaller particles are responsible for the long periods of dust haze in arid areas. The harmattan haze of equatorial Africa is an example of dust remaining aloft for extended periods of time.

There have been studies to determine dust particle sizes in particular areas, each of which features particles of specific chemical composition and size. Although some areas are similar, each usually has some special characteristics that make that it unique. Hooch (1984) provides some general particle categories. He puts clay at less than 2 microns; silt at between 2 and 74 microns; and sand/gravel at greater than 74 microns. This would suggest that blowing dust is composed largely of silt, and that generally, no clay is lifted. The larger particles fall into the sand and gravel range.

Studies conducted at Yuma Proving Ground by Greveris (1977) stratified particle size by composition. Greveris showed that the composition of dust particles with diameters less than 40 microns was 82% clay, gypsum, and carbonates; 18% was quartz. Particles larger than 40 microns were 69% quartz; 31% was clay, gypsum, and carbonates. Similar studies in Israel by Ganor (1975) as quoted by Gerson et al. (unkn) revealed that silt (2-74 microns) composition in the Negev Desert was 30-45% quartz, 30-50% calcite, 10-20% dolomite, and 5-15% feldspars. The hills in Israel were found to be rich in kaolinite (white clay of aluminum silicate), which was replaced in the more arid environments by montmorillonite (a type of clay consisting of aluminum silicate in which the aluminum may be replaced by magnesium). These substances are the primary reasons for clay's small particle size.

While other arid areas may have soils of similar composition, there are wide variations. For example, the pure gypsum of extremely small particle size found at White Sands, New Mexico, contrasts sharply with the rest of the Tularosa Basin, which is composed of gritty sand.

Without detailed particle size information, making firm assessments about lifting and settling in a given area must be based on experience rather than scientific method. Earlier, a preliminary soil analysis of eastern Saudi Arabia showed that there was no clay there, but that there was more sand than in the Negev Desert sample, which proves that larger particles settle out first, while smaller particles are carried farther south.

The effects of particle size on visibility remains an elusive quantity. A formula of these effects was developed in Sudan and Egypt with some success, but the correlation was lost when it was tested in other areas. Airborne dust tends to scatter and refract light (Hooch, 1984); the more uniform the dust content in the air, the more refraction. As dust particles settle within an airmass, particles of similar sizes refract light much as ice crystals produce halos and coronas. Suspended dust lowers slant range visibility when the sun angle is low (at sunrise and sunset), but visibility is better with higher sun angles or when the observer looks vertically through the dust cloud.

4.4 RULES OF THUMB FOR SAND/DUST FORECASTING

1. The lifting threshold for fine dust particles is 15 knots.
2. The average height of a duststorm is from 3,000 to 6,000 feet.
3. Temperatures in satellite imagery show that the tops of stronger duststorms reach to between 10,000 and 18,000 ft. The climatological temperature for those levels, therefore, is the temperature required for the top of the enhancement slope in a satellite enhancement curve.
4. The base temperature on an enhancement slope for a satellite enhancement curve is the surface "skin" temperature for the area of interest. Note that this "skin" temperature is NOT the free air (or shelter) temperature given in surface weather observations, but the satellite-determined temperature of the ground in sunlight. It is frequently 10-15 degrees higher than the air temperature.
5. Blowing or suspended dust settles when winds drop below the settling threshold of 15 knots.
6. Suspended dust generally settles at a rate of 1,000 feet per hour. This rate can be used to determine the time required to clear the air of dust particles and restore visibility. The settling occurs in the area to which the dust cloud has been advected. Frequently, source areas clear instantly when winds drop below the threshold speed.
7. Blowing dust does not usually occur for 24 hours after a rainfall if the ground is sufficiently dampened. A sustained wind dries the ground faster if the pressure gradient is maintained.
8. Haze and suspended dust associated with extreme storms have been reported as high as 35,000 to 40,000 feet.
9. When thermal low pressure associated with the Monsoon Trough is over southern Saudi Arabia, duststorms run in a 3-day cycle as new dust is lifted in Iraq every day to travel southward. The dust does not settle, but continues to advect southward into the cyclonic circulation, which is usually visible on satellite imagery and covers most of the Arabian Peninsula with dust.
10. Visibilities in blowing dust are usually between 0 and .5 nm in or near a source area. On the edges of blowing dust, and downstream for 100-150 miles, visibilities are .75 to 3 nm. As the suspended dust settles, visibilities usually return to 2-5 nm.

11. Duststorms associated with cold fronts are capped by the frontal inversion.
12. Summer shamal-type duststorms are generally capped by an inversion (frequently called a "turbulence inversion") created by mixing in the lower layers of the atmosphere. Heights average 1,500-6,000 feet.
13. Rapid heat loss due to nocturnal radiation helps lower the inversion to the surface and settles the dust.
14. Duststorms are usually cut off at the source area near sunset.
15. Blowing or suspended dust produces massive amounts of refraction and makes light sources appear several times larger than normal or creates a glow within the dust cloud.
16. Suspended dust is sorted by particle size into fairly homogeneous zones in the atmosphere, creating areas capable of reflecting and refracting light sources into unique patterns that may be misinterpreted as other objects. Halos, coronas, and sun dogs are examples of this phenomenon as it results from evenly distributed water/ice particles in the atmosphere.
17. Most duststorms originate in specific source areas that can be identified in satellite imagery--see Part 3. These source areas generate duststorms on a recurring basis whenever conditions for lifting the source material are met.
18. Source areas in the Middle East are generally lighter in color on satellite imagery than the surrounding terrain. The lighter color indicates that these sources are probably composed of salt and gypsum, common minerals in deserts due to high evaporation rates. Dry lake beds and the caps of underground domes of salt and gypsum (normally found in areas of large-scale oil production) are also lighter in color.
19. Dust devils, a small-scale hazard in desert areas, usually first occur in late March or April. Rules of thumb for occurrence are: 3 days without precipitation, temperature above 80° F, a very weak gradient that allows winds to be light and variable (generally less than 5-8 knots), and finally, clear to scattered skies. Once formed, these small cyclones can generate strong updrafts to lift dust and other loose objects. Dust devil winds are usually 15-25 knots, but 40-50 knots have been reported. Direction of travel is generally upslope. Dust devils can exceed several thousand feet in height. Unless dust or loose debris is present, these cyclones are difficult to spot; they can be a serious hazard to aircraft landing, taking off, or taxiing.
20. Blowing dust occurs in a zone of maximum winds in the lower levels of the atmosphere associated with converging jet streams at 200-250 mb. Usually, the polar and subtropical jet streams merge as an area of low pressure moves into a region. Frequently, the converging jets are in the southern to southeastern quadrants of the low-pressure area. To identify the area of strongest winds and blowing dust, track this convergent area to the surface toward the cooler air (toward the northeast).
21. Duststorms create the potential for large electrostatic discharges; to prevent damage, ground everything.
22. This is a simple lifting threshold table; note that traffic, whether by people, animals or vehicles, lowers thresholds. The areas known as "playas" in the United States are called "sabkhas" in the Middle East (Walker, 1986).

Fine to medium sand in dune-covered areas	10 to 15 MPH
Sandy areas, poorly developed desert pavement	20 MPH
Fine material, desert flats	20 to 25 MPH
Alluvial fans, crusted playas	30 to 35 MPH
Well developed desert pavements	40 MPH

23. This is a table of thermal contrasts for onset intensities of the winter shamal (Peer, 1984):

30 knots for Delta T = 10° C
35 knots for Delta T = 15° C Average gusts 10 knots greater.
40 knots for Delta T = 20° C Peak gusts 15-20 knots greater.
45 knots for Delta T = 25° C

24. The likelihood of duststorms is increased at least five times by large-scale military operations in the desert; this was a lesson learned from the 1940's British desert campaign in the North African Sahara, as footnoted in NAVENVPREDRSCHFAC Technical Bulletin 80-02, 1980.

25. The presence of a nocturnal jet of 30 kts or greater between 1,000 and 3,000 feet signals the onset of a summer shamal outbreak. This graph (from Membery, 1983) will help in forecasting the presence of the nocturnal jet.

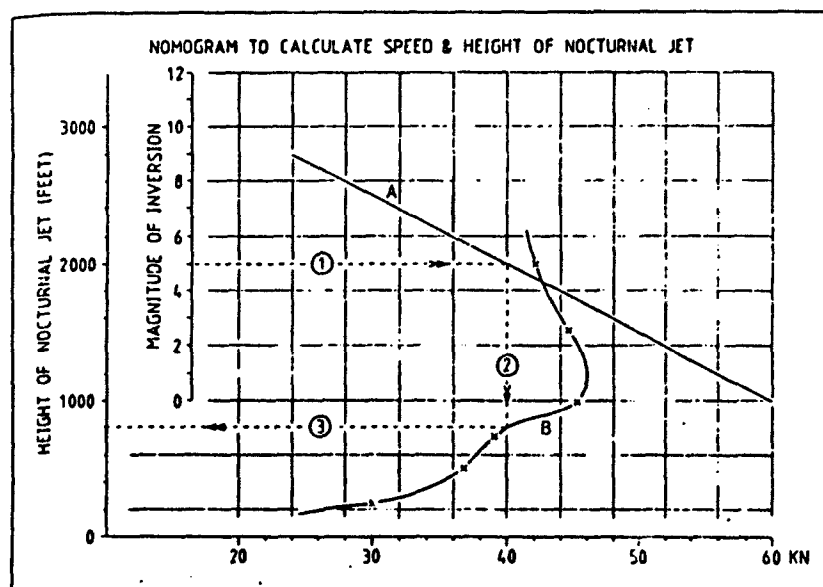


Figure 4-1. Nomogram to be used for forecasting speed and height of the nocturnal jet. (Membery, 1983). Straight line A is compiled from 98 data points; curve B, from 86 data points. Step 1: Forecast magnitude of inversion (e.g., 5° C) and locate intercept with A. Step 2: Read off speed of low-level max--40 knots. Step 3: Read off most probable height of max--800 ft. Valid for inversions 3° C < T < 9° C and for speeds 24 < S < 46 knots.

5. ENHANCING THE APPEARANCE OF DUST IN SATELLITE IMAGERY

Satellite imagery is unrivaled for providing information about synoptic weather features and severe weather potential (Anthony, 1977). It is also important in the detection of blowing dust, but there is a problem with interpretation of the dust features. Since dust is a surface-based phenomenon, the thermal contrast for detection by the infrared window is very small, resulting in a small degree of change in appearance on satellite imagery. In the satellite's visual window, the amount of dust detected varies depending on the terrain the dust is advected over. Dust over a dark body of water, for example, provides a good dust signature in visual imagery. But dust over land is less obvious because the dust cloud and the surface have the same basic coloration. Time of day also affects visual imagery; a low sun angle results in increased refraction in the dust and creates a three-dimensional effect, with shadows over the top and sides of the dust. A high sun angle results in less refraction and lends a transparent tendency to the dust cloud. The solution to dust detection problems, then, lies in learning how to enhance satellite imagery. There are several ways to do this. One way, effective with direct readouts, is to enhance the infrared window to increase the contrast and detail in areas where the dust might be found. Other methods, which include making composite imagery and histogram curves, require a computer to manipulate the data.

5.1 LITHOMETEOR ENHANCEMENT CURVES FOR ORBITING SATELLITES

The detection of lithometeors by satellites is difficult for two reasons. The first is that satellite sensors are designed to detect water vapor, and lithometeors (i.e., sand and dust) are dry. Second, lithometeors are usually confined to a thin layer near the surface, where thermal contrast is minimal.

The ability to manipulate satellite imagery to enhance a desired section of the imagery requires that the manipulator know exactly what needs to be enhanced and how to convey that information to the readout equipment. The concept is easy. The infrared sensor on the satellite works on a scale from hot to cold, which is depicted in shades of black to white. "Normal" imagery has a gentle, gradual slope at about a 45-degree angle from hot (black) to cold (white). To enhance a section of imagery, that section must be slanted more toward the vertical. The same spectrum of colors is available, but the spread of temperature is reduced, thus creating the enhancement. Once the required temperatures to be enhanced are known, they must be converted into input values that the machine can understand. Input values range from 0-255, but different sensors have different input values for the same temperature. The output values, which tell the equipment what color to produce, also range from 0-255. On the NOAA satellite, 0 is black and 255 is white--see Figure 5-1.

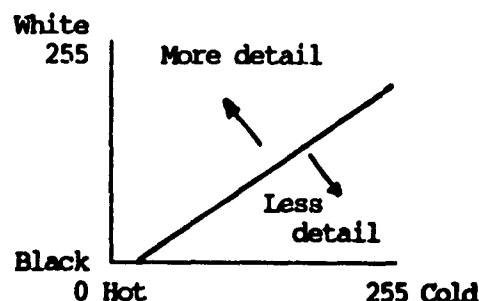


Figure 5-1. Example NOAA enhancement curve.

To eliminate the thermal contrast problem, the enhancement curve must have a steep slope of enhancement that confines the image to a very small thermal window. The key to this enhancement curve is to base the bottom (warmest) temperature as close as possible to the seasonal surface temperature of the area of interest. Consideration must also be given to the time of day the orbiting satellite passes over area of interest. By doing this, the section of data thermally enhanced is the layer closest to the earth's surface where lithometeors occur most. The steeper the enhancement slope, the smaller the thermal window and the more detailed the imagery. With the smaller thermal window, however, it is harder to keep the window aligned with surface temperatures, especially during seasonal transitions or with large geographic temperature contrasts. For the best results, temperatures should be fine-tuned daily.

Since the original enhancement technique was developed by NOAA, and since the maximum occurrence of blowing dust/sand is in the afternoon, NOAA9 was used to implement the enhancement curves because it had a mid-afternoon nodal crossing. All the imagery used was Channel 4 infrared (IR) data from NOAA satellites. The curves also work on DMSP satellites, but poor nodal time crossings for lithometeor detection and a smaller thermal range in the IR channel require more detail in the enhancement curve for adequate dust detection.

The original NOAA enhancement curve had a thermal window from $+30^{\circ}\text{C}$ to $+10^{\circ}\text{C}$. This curve, used in the early summer, showed the blowing dust slightly better than unenhanced IR data. But under closer examination, the curve was too cool for the extreme temperatures of the Middle East. The bands of dust appeared to be enhanced at about the gradient level--see Figure 5-2.

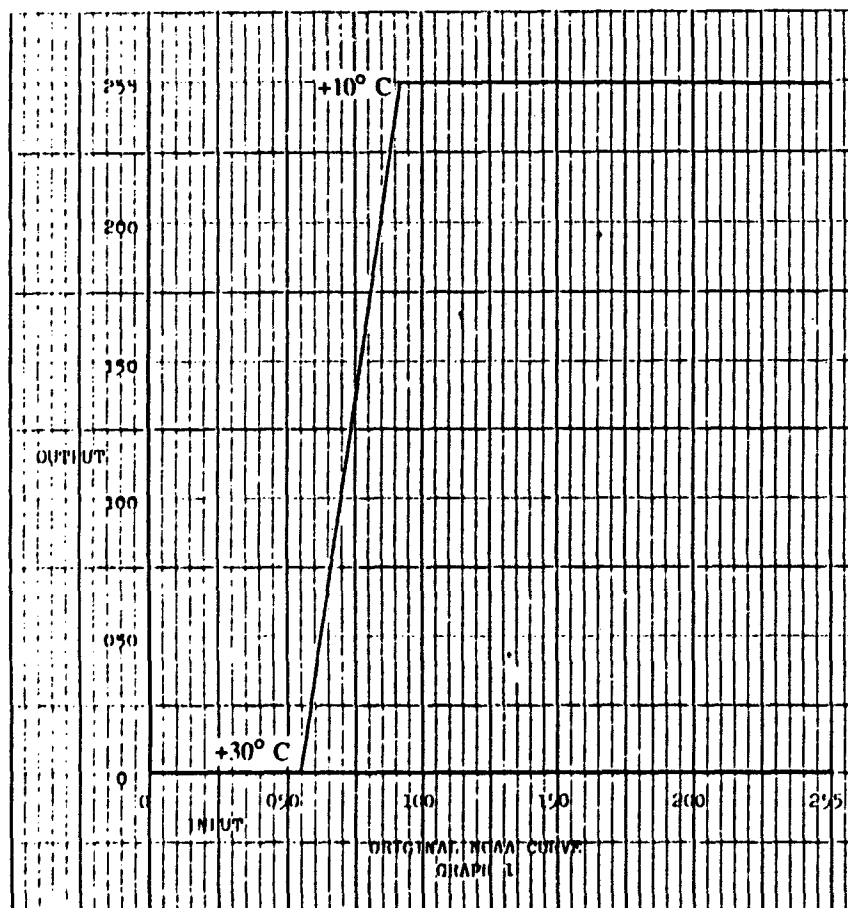


Figure 5-2. Original NOAA enhancement curve.

To detect surface dust better, the base temperature of the enhancement slope was moved out to $+38^{\circ}\text{C}$ while the top of the slope was maintained at $+10^{\circ}\text{C}$. This curve showed remarkable detail and worked extremely well through the summer months. Usually, the amount of sand detected was three to five times as much as on unenhanced IR imagery. Small-scale circulations can be detected in the enhanced sand patterns, revealing small anticyclones and cyclones. This imagery provides excellent additional input to conventional surface analysis techniques, especially in data-sparse areas. The most notable problems with the summer curve were that coastal and vegetated areas are substantially cooler, resulting in a distorted appearance because of the moisture and cooler air. Also, because there is no slope that provides data cooler than $+10^{\circ}\text{C}$, all data cooler than $+10^{\circ}\text{C}$ is "bleached out"--see Figure 5-3.

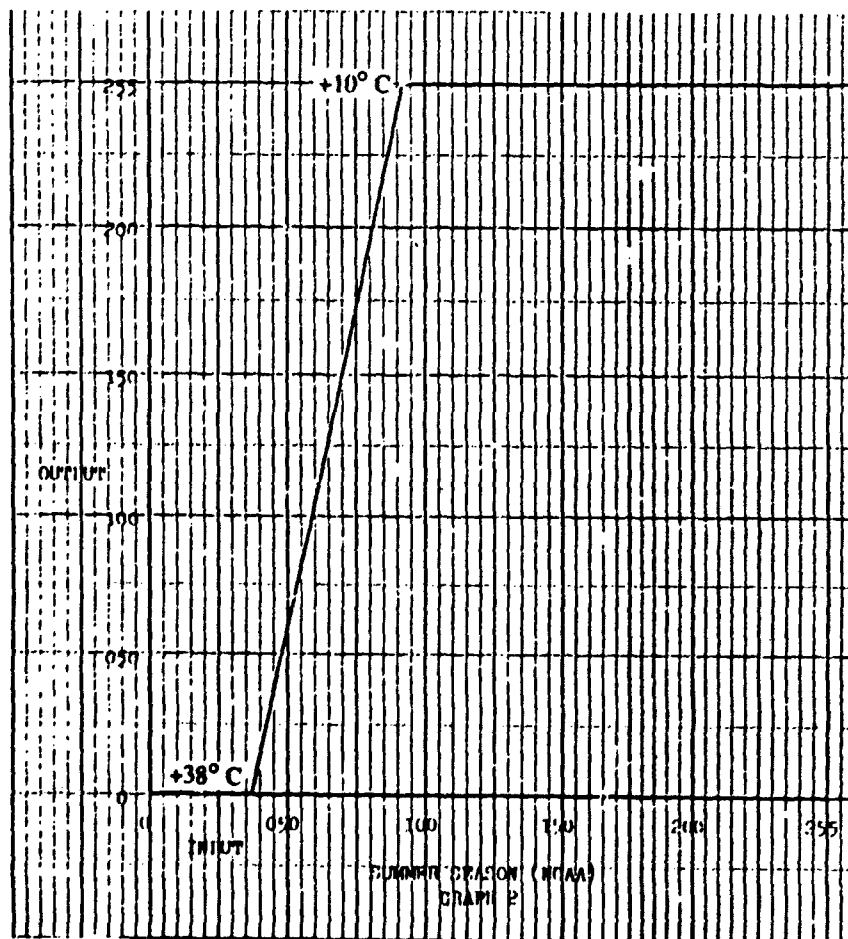


Figure 5-3. NOAA summer season curve.

The best enhancement, developed for midsummer NOAA use, doubles as the winter curve for DMSP imagery. The base temperature was extended to $+47^{\circ}\text{C}$ with a gradual slope up to $+30^{\circ}\text{C}$, then sloped sharply up to $+5^{\circ}\text{C}$ for dust enhancement. This curve has a second slope that drops back to $+4.5^{\circ}\text{C}$, then slopes slowly up to -40°C to bring back detail in the cooler areas of the imagery (higher clouds or cooler terrain). This imagery offers sharp detail of surface features across desert areas, good depiction and detection of mid-day dust, and good depiction of middle and high clouds. The basic concept for deriving enhancement slope temperatures was to use the climatic temperature across the desert at the NOAA nodal crossing for the base temperature ($+47^{\circ}\text{C}$). Because the author's experience showed that the denser dust "cloud" was usually below 10,000 feet, but occasionally higher, 500 mb (18,000 feet) was selected as the top temperature for the slope ($+5^{\circ}\text{C}$). These temperatures could be altered to fit daily temperatures in an area of interest area, with favorable results. As mentioned earlier, if the temperature range

is narrowed ($+47^{\circ}\text{C}$ to $+5^{\circ}\text{C}$), sharper detail is noted--see Figure 5-4. Corresponding temperatures for the DMSP were $+27.44^{\circ}\text{C}$ for the base, sloped gradually to $+11.44^{\circ}\text{C}$, then up sharply to -12.09°C . A drop to -12.56°C with a slow increase to -50.68°C provides a good view of middle and high cloudiness, as well as a look at cooler areas, including post-frontal air masses.

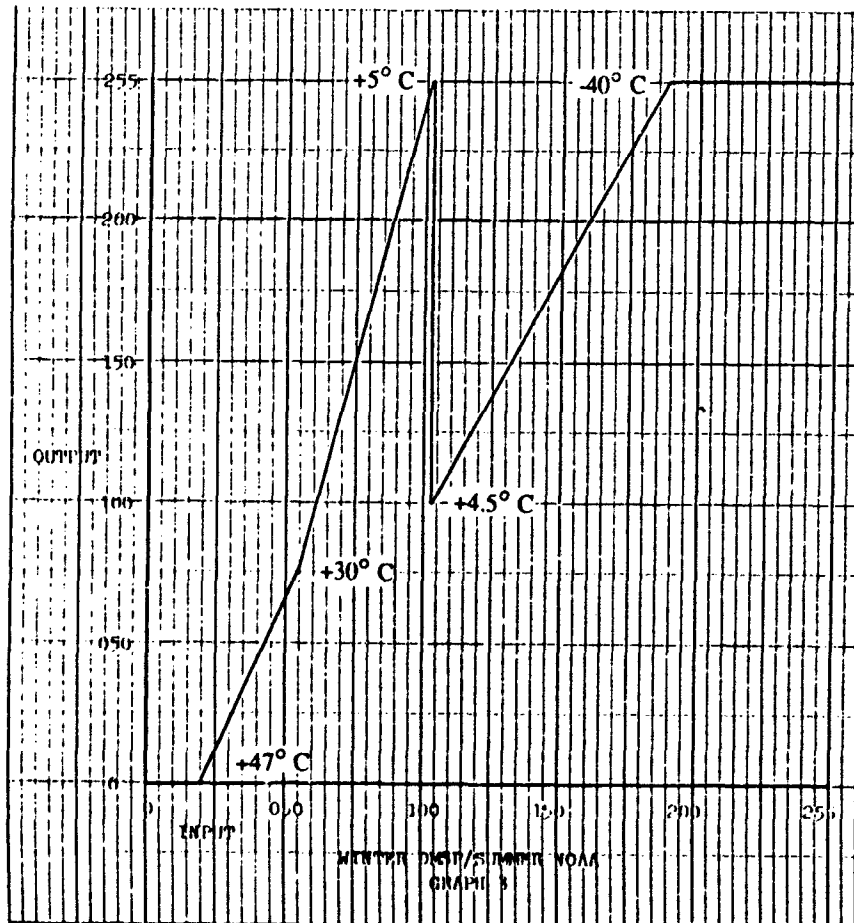


Figure 5-4. Winter DMSP/summer NOAA.

By autumn, surface temperatures cool to the point at which dust is lost between slopes; surface temperature on the enhancement needs to be lowered to $+30^{\circ}\text{C}$, with the top at $+5^{\circ}\text{C}$. To keep the cooler data visible, the slope was extended from $+4.5^{\circ}\text{C}$ to -37°C , with flat areas between -15°C and -20°C and between -28°C and -33°C to enhance jet-stream cloud decks. This curve worked extremely well through the autumn until still cooler temperatures again distorted surface detail and dust depiction. Anomalies such as large sheets of surface area changed colors as temperatures fell between slopes. The usual white appearance of the dust suddenly reverse to dark gray when the dust moves over water at a coastline. This was assumed to be caused by contamination of the satellite sensor by relatively warmer water temperatures--see Figure 5-5.

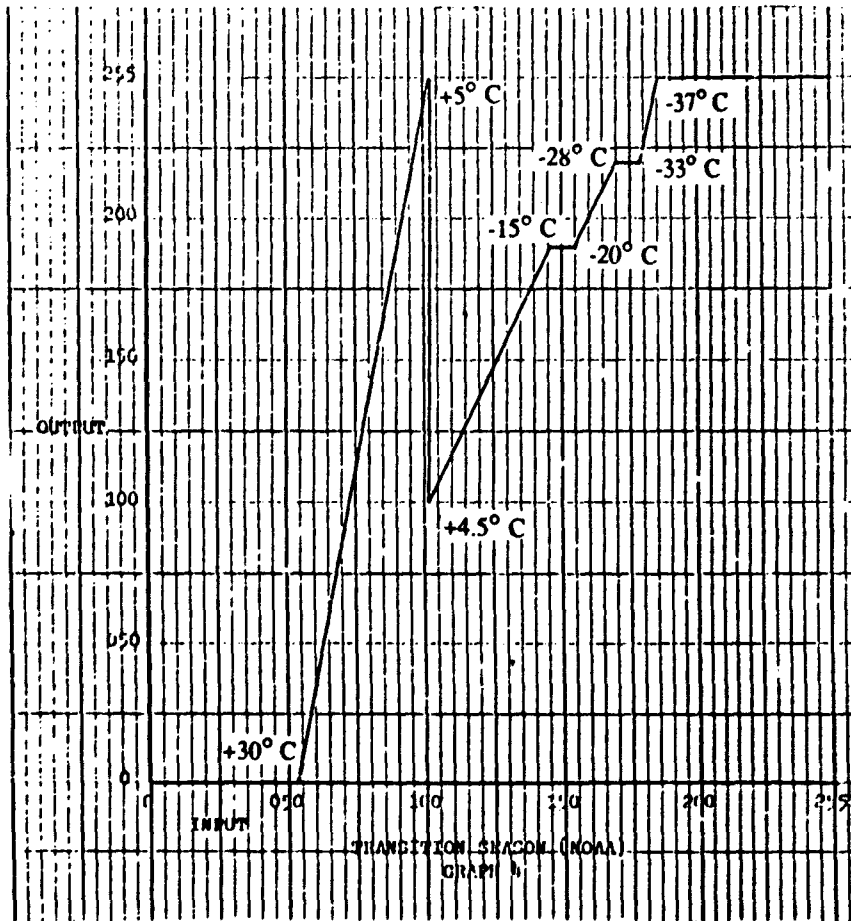


Figure 5-5. NOAA transition season enhancement curve.

These curves can also be used at different times of the day by matching temperature ranges of the curve to that time of day. This allows for the acquisition of some useful data, particularly in the evening and at night when the cooler land does not show much contrast due to radiational cooling. The contrast between warmer water and the cooler dust plume will reflect well, however.

The winter enhancement curve (Figure 5-6) lowers the base temperature to $+27^{\circ}\text{C}$ to retain as much detail as possible in the southern deserts; this temperature is still low enough to work in the cooler air over North Africa and the Middle East. Some detail is lost over the equatorial area, however, as the temperatures are too low. The top of the slope was put at -10°C using the assumption that surface temperatures would not be lower than from $+5^{\circ}\text{C}$ to $+10^{\circ}\text{C}$ across most of the region. The additional cooler slope was kept from -10.5°C to -60°C . The winter curve can double as a nighttime enhancement for NOAA imagery.

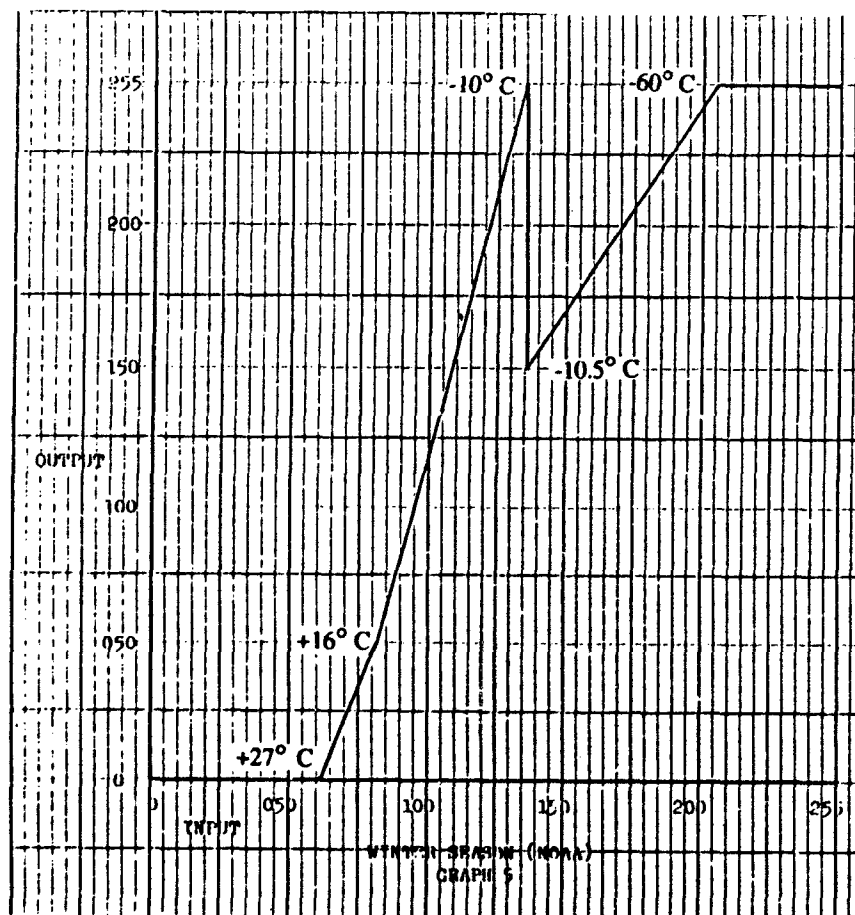


Figure 5-6. NOAA winter enhancement curve.

The winter curve brings back most of the sand detail across the desert areas, with improved detection in the cool sector. The wide temperature range during winter forces the analyst to decide which data is more important--that from the southern or the northern portion. Although some modification can be done, be careful not to flatten the sand slope or some detail will be lost. With this curve, lowering temperatures to about a base of +15° C further enhances the cold air section (such as behind fronts) to bring out more contrast in the dust and surface detail. This sacrifices data in the south, however.

The first attempts at converting NOAA enhancement tables for use with DMSP began with F-8 data. DMSP imagery has a smaller thermal window than NOAA imagery, a fact that causes problems in trying to convert the imagery to the enhancement curves. The DMSP transition curve base temperature is +11.44° C as compared to NOAA's +30° C. The top temperature of +5° C for NOAA became -12.09° C for DMSP. The DMSP F-8 imagery was enhanced to the point of appearing like thermal fine data in the cold sector, while the warm sector was obviously blacked out with the base temperature of +11.44° C.

The corrected winter curve for DMSP imagery, discussed earlier, was shown in Figure 5-4. This curve tested successfully on both DMSP F-8 ATS in the morning hours and DTS in the evening hours. It also tested well on DMSP F-9 DTS data in the late night hours. It was also successfully tested and used as a transition season nighttime curve. Again, use caution in interpreting nighttime imagery; the nocturnal radiational cooling in the boundary layer of the atmosphere reduces the contrast between land surfaces and blowing dust.

The final curve developed was the DMSP summer enhancement shown in Figure 5-7. This curve was tested on DMSP F-9 ATS in the late morning hours. The base temperature was set at the highest possible for F-9 ($+36.4^{\circ}\text{C}$) with the characteristically steep slope to $+10.5^{\circ}\text{C}$. A second slope from $+10.0^{\circ}\text{C}$ to -40.3°C allowed for detail in the lower temperatures. Nodal times on F-9 made it unreliable for finding dust, except for early detection of the dust plume associated with the summer shamal.

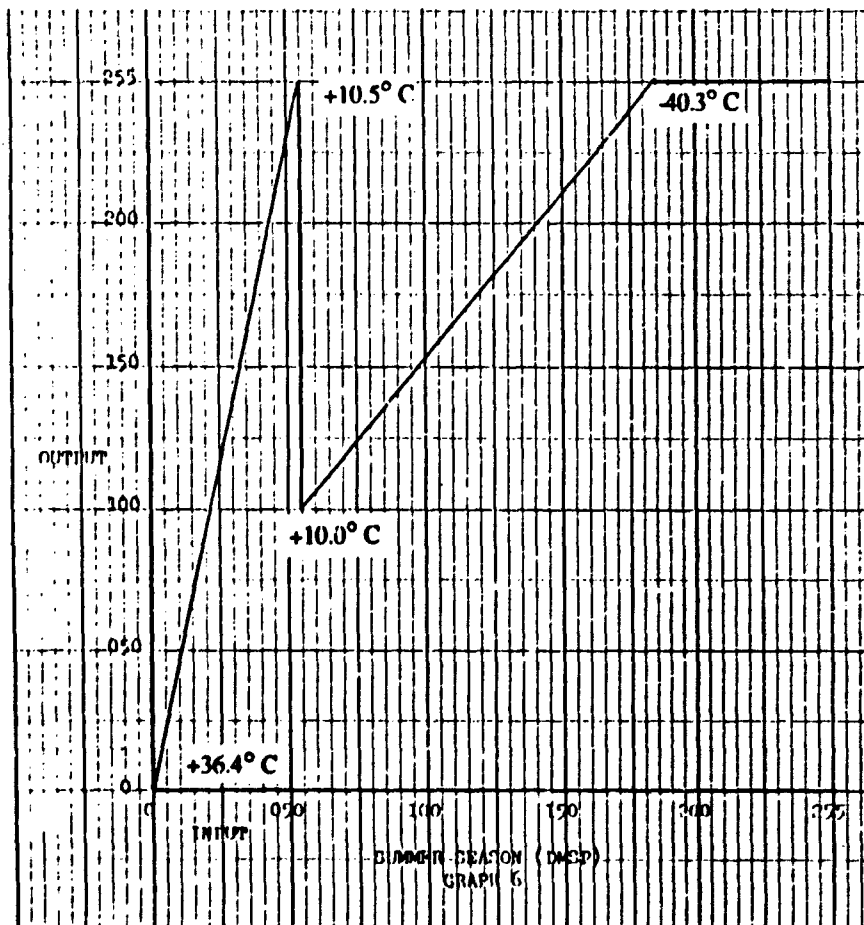


Figure 5-7. DMSP summer enhancement curve.

One of the keys to using enhanced imagery successfully is to keep a control set for distinguishing geographical features from dust signatures. Ideally, one cloud-free view in each channel should be set aside to detect extraordinary features. If an unusual feature is noted in the infrared, it, too, can be checked against the control set to see if it is a permanent terrain feature or a thermal irregularity at the surface.

5.2 COMPOSITE IMAGERY

Another way of enhancing the appearance of blowing dust on satellite imagery is by taking advantage of different satellite channels. Although visual imagery produces a good dust signature over a darker water body, it doesn't show much over land, where the color of the dust closely matches terrain. On the other hand, the thermal imagery can detect a dust plume over land to a fair degree because the lifted dust appears slightly cooler than the desert surface below. When dust moves over water, the lower sea surface temperature closely matches the temperature of the dust cloud, making detection difficult, even impossible. A technique for merging the two channels into a single composite image (Lee, 1989) allows the best of the two images to be used.

Composite images are created by an image processing station, where an imaginary line can be placed at the coastline to separate the imagery. In the visual image, all data over the land mass is eliminated or blacked out by reducing all pixels of data to 0. In the infrared image, the same procedure is performed to eliminate all the data over the water body. The two half images are then merged, pixel by pixel, to form a composite that reveals a continuous image of the dust plume extending from the land and over the water.

The composite image is not enhanced; it simply takes the best portions of both pictures to provide a useful image. Another use of this technique would be to run one enhancement curve for the land-mass temperatures and a second for the water body (to match its cooler temperature), then merge the two to produce a continuous enhanced image. Still another option would be to run separate enhancement curves in front of and behind a frontal system to match the air mass temperatures, then merge them to form a composite.

5.3 HISTOGRAMS

The histogram is another type of linear contrast enhancement performed on satellite imagery. The process is done usually by an imagery processing station, but some small computers are capable of it as well. The procedure enhances a selected section of a satellite image using a full spectrum of contrast (0-255) on a smaller area. It is relatively quick and easy. The image can be quickly enhanced to show the features of a warm sandstorm, then changed to show another feature. The enhancement is not based on temperature; instead, the original image's contrast is expanded to increase the detail. The enhancement slope extends from 0 (a near vertical slope of maximum enhancement) to 100, which is a small angle off the horizontal, with minimum enhancement. The slope can be adjusted to any value between 0 and 100. The versatility of this procedure is speed with which it can convert from one enhancement to another. If enhancement is needed in a warm section of the imagery, that area is simply specified to the computer and the enhancement is made. If, for example, the designated section only had black (0) and medium gray (125) shading, the black is still black (0) and the medium gray is now white (255) after the enhancement is run.

This procedure can be used for all types of imagery because a thermal radiometric table is not required to base temperatures on. This expands the application to most satellite types received and input into the system. In addition to thermal data, the procedure can be used in visual imagery to enhance available light and make the imagery useful during low sun angle periods (sunrise or sunset). It is also helpful in increasing contrast in moonlight visual imagery.

6. EXAMPLE SATELLITE IMAGERY--THE WINTER SHAMAL



Figure 6-1. Blowing dust associated with a moderate cold front across the northern Persian Gulf and northeastern Saudi Arabia. In this midday imagery, observing the dust is difficult except over the water. The density of the dust along the front, however, makes it visible over the desert in eastern Saudi Arabia. DMSP F7 ALFR+9 19/0607Z OCT 1984 REV 4771 NODAL 60.98E.



Figure 6-2. The blowing dust from Figure 6-1 is shown here 3 days later. The dust has pushed southward with the cold front into the northern Arabian Sea. All that remains of the frontal cloudiness is a narrow rope cloud over the water. A cyclonic circulation is evident in the dust near Masirah, Oman. Denser plumes of dust can be seen blowing off the southern coast of Iran into the Gulf of Oman. DMSP F7 ALF R+8 22/0506Z OCT 1984 REV 4813 NODAL 76.15E.



Figure 6-3. A strong cold-front-generated sandstorm can be seen moving from Iraq and northern Saudi Arabia toward the southeast. The sand is so dense that surface features are totally obscured. DMSP F7 R+9 ALS 16/0614Z APR 1984 REV 2130 NODAL 39.27E.

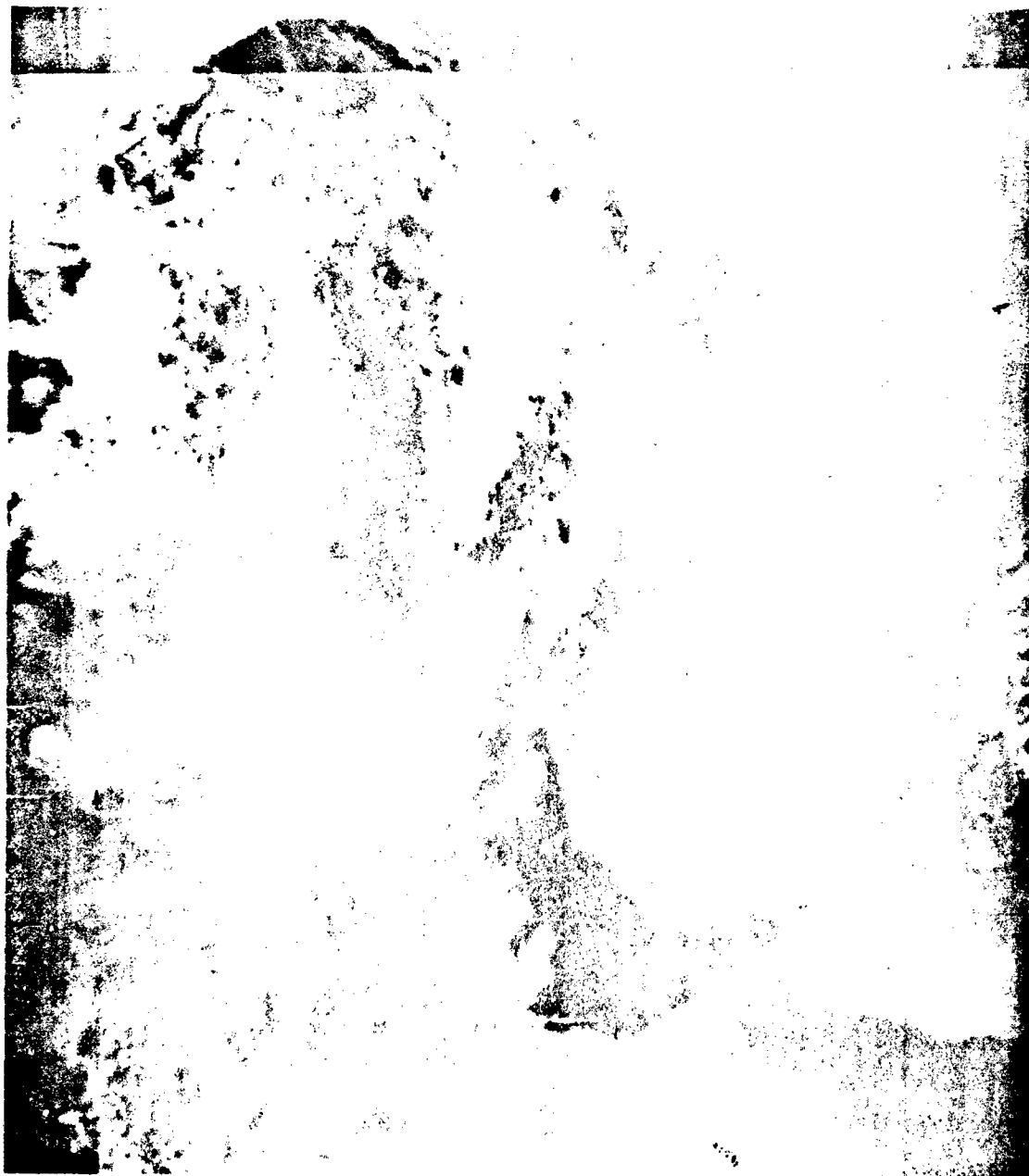


Figure 6-4. The afternoon image of the strong spring cold frontal sandstorm shown in Figure 6-3. It now shows the storm, with a smoky opaque appearance, covering most of the northern Arabian Peninsula. Where plumes are visible, they extend from the southwest to northeast even though the duststorm is postfrontal. Along the leading edge of the front, cumulus is forming over northeastern Saudi Arabia. To the north, Lakes Tharthar and Milh in central Iraq are fairly clear. NOAA7 R+11 ALS 16/1142Z APR 1984 REV 14515 NODAL 57.68E.



Figure 6-5. The Infrared (IR) version of Figure 6-4 shows both the extent of the dust and the cumulus formation better. Dust plumes are more obvious across the northern peninsula. They appear to follow the 500-mb flow closely, with the trough extending just west of the plumes. Note the cirrus over the Red Sea moving toward the southeast. NOAA7 R+11 ATS 16/1142Z APR 1984 REV 14515 NODAL 57.68E.



Figure 6-6. A normal IR shot across central Africa shows the extent of blowing dust/sand associated with the almost permanent winter shear line in this area. Note Lake Chad just to the south of the sand. Cooler air is seen as the lighter shaded areas to the northeast of the front. NOAA9 R+13 ATS 27/1306Z DEC 1985 REV 5362 NODAL 21.62E.

7. EXAMPLE SATELLITE IMAGERY--THE SUMMER SHAMAL



Figure 7-1. Narrow plumes of dust are seen in the early stages of a summer shamal duststorm in southeastern Iraq. The plumes originate from pinpoint source regions in Iraq and extend southward into Kuwait and the northern Persian G. If. These plumes are sometimes difficult to locate on light data, but are easily detected in this IR image. NOAA7 R+11 ATS 08/1144Z AUG 1984 REV 16125 NODAL 60.03E.



Figure 7-2. The IR version of the image in Figure 7-1 detects the light colored plumes of dust in Iraq moving over the moister and darker shaded surface areas. Note the sunglint on Lakes Tharthar and Milh in Iraq, and along the eastern shores of the Tigris River near Baghdad. NOAA7 R+11 ALS 08/1144Z AUG 1984 REV 161257 DAL 60.03E.



Figure 7-3. An afternoon light shot across the Arabian Peninsula showing the typical summer shamal plumes extending from southeastern Iraq to the south into Kuwait and the northern Persian Gulf. Dust can also be seen blowing off the horn of the peninsula toward the west into the Persian Gulf. More dust is seen extending into the northern Arabian Sea. Note the sunglint to the northeast of Cyprus. A single CB can be seen over the Hajar Mountains. NOAA' R+12 ALS 25/1200Z AUG 1987 REV 13910 NODAL 47.65E.



Figure 7-4. The normal IR counterpart of the image in Figure 7-3. It shows substantially more dust extending from southeastern Iraq and south across the eastern portions of Saudi Arabia, as well as over the eastern tip of the Arabian Peninsula. NOAA9 R+12 ATS 25/1200Z AUG 1987 REV 13910 NODAL 47.65E.



Figure 7-5. The enhanced IR image of the previous two images (Figures 7-3 and 7-4). It again increases the amount of dust that can be seen. In this shot, the dust extends farther north along the Euphrates river plains into central Syria. The general circulation of a large low-pressure area can be made out in southeastern Saudi Arabia just south of the Persian Gulf. NOAA9 R+12 ATS TW60 25/1200Z AUG 1987 REV 13910 NODAL 47.65E. Note: the enhanced portion of this shot is from 38° C to 10° C.



Figure 7-6. A sunset light pass shows a large-scale summer shamal duststorm at full strength. The dust is still being lifted at the source areas in southeastern Iraq, as evidenced by the pinpoints at the windward edge of the dust/sand. The low sun angle again enhances the dust's appearance, but renders the eastern portions of the data almost useless. Note the bright spot in southern Iran just north of the Gulf of Oman. The vertical extent of a CB is still in the sunlight, while lower clouds have darkened, creating a bright area on one side and a shadow on the other. DMSP F6 R+1 DLS 27/1456Z JUN 1985 REV 13065 NODAL 51.34E.



Figure 7-7. An evening light pass showing a full-scale summer shamal duststorm in the eastern Arabian Peninsula. The source areas in Iraq are still active. The low sun angle has enhanced the roughness of the top of the plumes of dust/sand. Sunglint can be seen on Lake Milh in Iraq. DMSP F6 R+1 DLS 02/1458Z AUG 1984 REV 8390 NODAL 50.28E.

8. EXAMPLE SATELLITE IMAGERY--VORTEX



Figure 8-1. A well-developed duststorm over the southeastern Arabian Peninsula is seen circulating into a low-pressure area in the Monsoon Trough. Although the low sun angle of this sunrise ascending light fine satellite shot aids in observing the dust, it creates problems on the edges of the pass where glare obscures the data. F6 ALF R+9 25/0258Z JUN 1985 REV 13080 NODAL 50.67E.



Figure 8-2. A nighttime pass under a full moon creates some excellent visual imagery. The presence of a major duststorm circulating into a low-pressure area associated with the monsoon/thermal trough can be seen in central Saudi Arabia. Note the abundance of stratus along the southeastern Arabian coast and Pakistani coasts; this is associated with cold water upwelling in the northern Arabian Sea induced by the strong southwest monsoon windflow. DMSP F7 R+1 DLS 25/1852Z AUG 1985 REV 9180 NODAL 48.81E.



Figure 8-3. A sunrise expanded light shot of a large-scale duststorm that has circulated into a low-pressure area associated with the monsoon/thermal trough over the southeastern Arabian Peninsula. Streaks of cirrus and associated shadows can be seen extending over the dust. Again, the low sun angle creates almost unusable imagery on the eastern edge. DMSP F6 R+9 ALF-X2 12/0258Z JUL 1984 REV 8085 NODAL 50.16E.



Figure 8-4. An afternoon light image across northwestern Africa shows little or no visible dust, but an area of slightly lighter than normal shading can be seen on the west side of the image.

NOAA9 R+13 ALS 18/1454Z AUG 1987 REV 13813 NODAL 6.78E.



Figure 8-5. The normal IR counterpart of the image shown in Figure 8-4 shows a narrow band of blowing dust on the west side of the imagery. This indicates enough curvature between the sand and cumulus to the east to aid in analyzing a low-pressure area. Dust also extends from the Spanish Sahara to the south along the west side of the low circulation. NOAA9 R+13 ATS 18/1454Z AUG 1987 REV 13813 NODAL 6.78E.

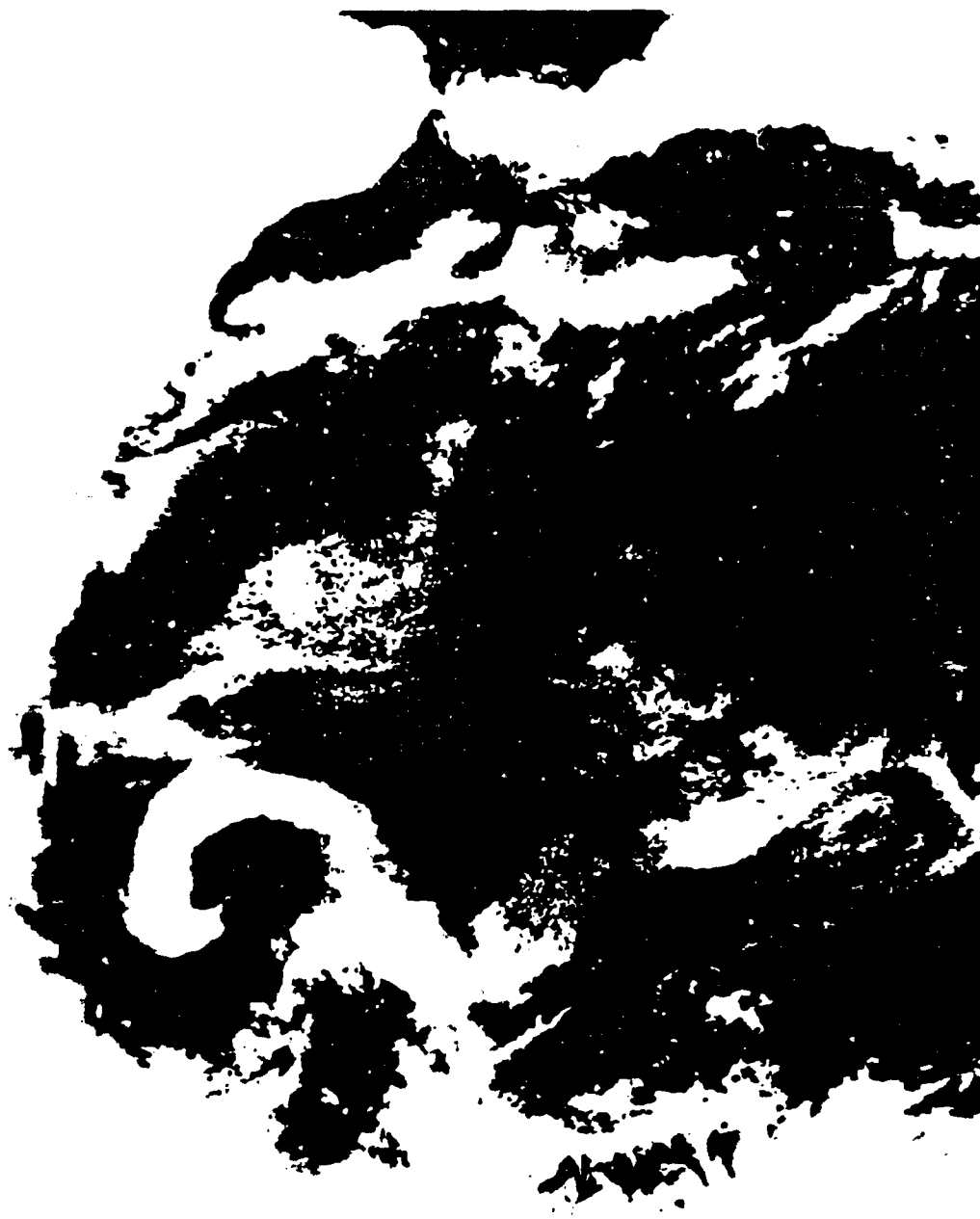


Figure 8-6. The enhanced IR of the previous two images (Figures 8-4 and 8-5) further increases the amount of dust that can be seen. This image shows a dramatic low-pressure circulation with dust blowing around a center comparable to the eye of a hurricane. NOAA9 R+13 ATS TW60 18/1454Z AUG 1987 REV 13813 NODAL 6.78E. Note: the enhanced portion of this shot is from 38° C to 10° C.

9. EXAMPLE SATELLITE IMAGERY--THE HABOOB



Figure 9-1. Thunderstorms generated by a weak frontal system in Iraq have created a haboob-style duststorm in southeastern Iraq. It is moving east toward Kuwait. DMSP F7 R+9 ALS 14/0714Z MAY 1985 REV 7711 NODAL 43.77E.



Figure 9-2. A light image over central Africa shows the size that downrush arcs can achieve. The downrushes have tremendous potential for blowing dust. Note Lake Chad to the north of the arc. DMSP F7 R+10 ALS 20/0836Z OCT 1986 REV 15153 NODAL 20.68E.

10. EXAMPLE SATELLITE IMAGERY--MOUNTAIN GAP



Figure 10-1. Dense dust is seen blowing from Sudan through the Tokar Gap into the Red Sea. A clear day with no sand or dust activity across the Arabian Peninsula makes a good control picture to compare to future blowing dust occurrences. DMSP F7 R+9 ALS 18/0652Z JUN 1986 REV 13391 NODAL 46.87E.

11. EXAMPLE SATELLITE IMAGERY--OTHER



Figure 11-1. A postfrontal enhanced IR image across the northern Arabian Peninsula. This was one of the early test images using the enhancement curves on DMSP imagery; the curve created detail on the surface comparable to fine imagery. Note the sharpness of the rivers, lakes, and terrain patterns in Iraq. The curve also picked up Baghdad, a dark spot showing the warmer city surrounded by cooler terrain. DMSP F8 R+9 ATS TW-61 29X0312Z DEC 1987 REV 2712 NODAL 44.76E.



Figure 11-2. An afternoon light image across northeastern Africa with no dust visible. Note the sunglint over the central Mediterranean Sea associated with high pressure to the north of Libya. NOAA9 R+12 ALS 02/1322Z JUL 1987 REV 13149 NODAL 25.47E.



Figure 11-3. The normal IR counterpart of the image in Figure 11-2. It is almost totally black from the extreme heat across the desert. Some dust is visible in northeastern Sudan. NOAA9 R+12 ALS 02/1322Z JUL 1987 REV 13149 NODAL 25.47E.

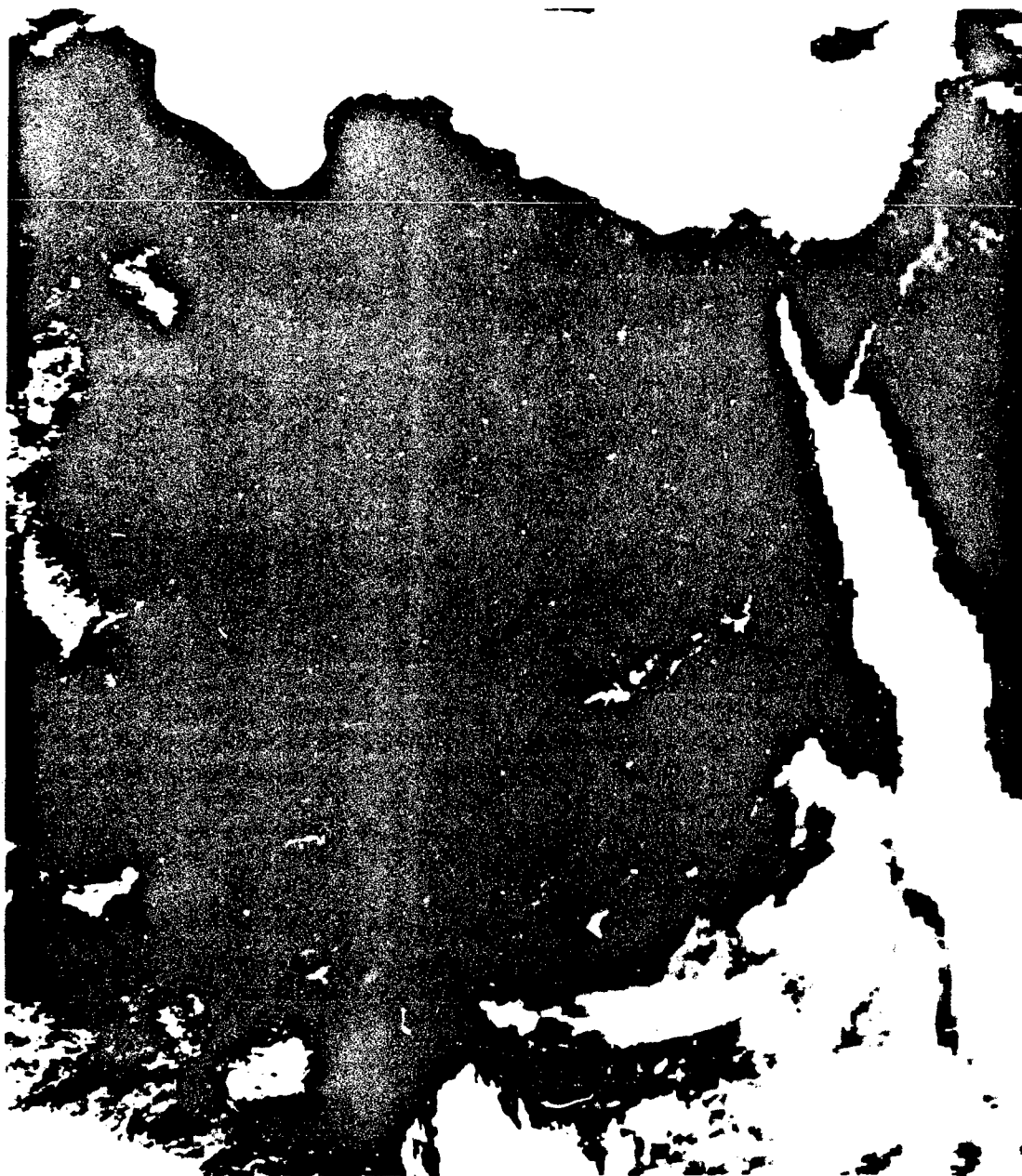


Figure 11-4. The enhanced IR version of the previous two images (Figures 11-2 and 11-3) increases the amount of dust visible. It also indicates several possible small-scale circulations in the dust, useful for analysis in Sudan. NOAA9 R+12 ATS TW60 02/1322Z JUL 1987 REV 13149 NODAL 25.47E. Note: the enhanced portion of this image is from 38° C to 10° C.

BIBLIOGRAPHY

- Anthony, Richard W., "Dust Storm - Severe Storm Characteristics of 10 Mar 1977," *Monthly Weather Review*, American Meteorological Society, Vol 106, No 8, pp. 1219-1223, Aug 1978.
- Atkinson, Gary D., *Forecasters' Guide to Tropical Meteorology*, AWS Technical Report (TR) 240, Scott AFB, IL, Apr 1971.
- Awad, Ali, *Dust Phenomena at Baghdad Airport*, from AWS Technical Library, 1990.
- Bagnold, R. A., *The Physics of Blown Sand and Desert Dunes*, Chapman and Hall, New York, NY, 1984.
- Berkofsky, Louis, "A Heuristic Investigation to Evaluate the Feasibility of Developing a Desert Dust Prediction Model," *Monthly Weather Review*, American Meteorological Society, Vol 110, No 12, pp. 2055-2062, Dec 1982.
- Blake, D. W., "Heat Low Over the Saudi Arabian Desert During May 1979," *Monthly Weather Review*, American Meteorological Society, Vol 111, No 9, pp. 1759-1775, Sep 1983.
- Brody, L. R., and LCDR M. J. R. Nester, *Handbook for Forecasters in the Mediterranean, Part 2, Regional Forecasting Aids for the Mediterranean Basin*, NAVENVPREDRSCHFAC Technical Report 80-10, Monterey, CA, Dec 1980.
- Coles, F. E., *Dust-Storms in Iraq*, Meteorological Office, Professional Notes No. 84, HMSO, London, 1938.
- Compton, Robert R., *Interpreting the Earth*, Harcourt Brace Jovanovich, Inc, New York, 1977.
- Corliss, William R., *Unknown Earth: A Handbook of Geological Enigmas, The Sourcebook Project*, Glen Arm, MD, 1980.
- Druian, Perla, and Louis Berkofsky, *Dust Storms at Sede Boqer*, Desert Meteorology Papers, Ben Gurion University at the Negev, Israel, Jan 1983.
- Foster, Robert J., *General Geology*, Charles E. Merrill Publishing Company, Columbus, OH, 1969.
- Fujita, T. Theodore, *The Downburst, Microburst and Macrobust, Report of Projects NIMROD and JAWS*, Chicago, 1986.
- Fujita, T. Theodore, *DFW Downburst On August 2, 1985*, Chicago, 1986.
- Gerson, Ran, Rivka Amit, and Sari Grossman, *Dust in Soils With Special Reference to Arid Terrains*, The Hebrew University, Jerusalem, Unkn.
- Gillette, D. A., "Environmental Factors Affecting Dust Emission by Wind Erosion," *Saharan Dust, Mobilization, Transport, Deposition, SCOPE*, 1979.
- Greveris, Harry A., *Desert Environmental Handbook*, U.S. Army Yuma Proving Ground, 1977, reprinted as *The Effects of Desert on Man and Machine*, AWS/FM-100/015, Scott AFB, IL, Aug 1980.
- Henley, Ponder, *Unpublished soil sample report*, Remote Sensing Division, Research Institute, U.S. Army Engineer Topographic Laboratories, Ft Belvoir, VA, 21 Nov 90.

- Hoock, Donald, "A Survey of Available Data Characterizing the Battlefield Dust Environment," *Battlefield Dust Environment, Symposium I*, US Corps of Engineers, Washington, DC, Dec 1984.
- Idso, S. B., R. S. Ingram, and J. M. Pritchard, "An American Haboob," *Bulletin of the American Meteorological Society*, Vol 53, No 10, pp. 930-935, Oct 1972.
- Idso, Sherwood B., "Dust Storms," *Scientific American*, Vol 235, No 4, pp. 108-114, 1976.
- International Station Meteorological Climate Summary*, Naval Oceanography Command Detachment Asheville, USAFETAC OL-A, and National Climatic Data Center, Ver 1.0, Asheville, NC, Oct 1990.
- Joussaume, Sylvie, "Three-Dimensional Simulations of the Atmospheric Cycle of Desert Dust Particles Using a General Circulation Model," *Journal of Geophysical Research*, Vol 95, No D2, pp. 1909-1941, Feb 20, 1990.
- Kalu, A. E., "The African Dust Plume: Its Characteristics and Propagation Across West Africa in Winter," *Saharan Dust, Mobilization, Transport, Deposition, SCOPE*, 1979.
- Lee, Thomas F., "Dust Tracking Using Composite Visible/Ir Images: A Case Study," *Weather and Forecasting, American Meteorology Society*, Vol 4, No 2, pp. 258-260, Jun 1989.
- Lawson, T. J., "Haboob Structure - Sartoum," *Weather*, Mar 1971.
- Marcal, Georges, *Meteorology of the Persian Gulf and of Several Airports on the Arabian Coast*, FTD-ID (RS)T-0113-85, Foreign Technology Division, Apr 1980.
- Membery, D. A., "Low Level Wind Profiles During the Gulf Shamal," *Weather*, Vol 38, pp. 18-24, 1983.
- Middleton, N. J., "Dust Storms in the Middle East," *Journal of Arid Environments*, Vol 10, pp. 83-96, 1986.
- Miscellaneous Notes of Forecasting in Iraq*, Unknown author and publisher, Dec 1936 - Dec 1938.
- Morales, C., "The Use of Meteorological Observations for Studies of the Mobilization, Transport, and Deposition of Saharan Soil Dust," *Saharan Dust, Mobilization, Transport, Deposition, SCOPE*, 1979.
- Navy Tactical Applications Guide, Volume 5, Part 1, Indian Ocean, Red Sea, Persian Gulf, Weather Analysis and Forecast Applications*, Walter A. Bohan Co, IL, 1983.
- Peer, Richard G., *Southwest Asia (SWA) Weather Familiarity Training, Winter (Dec-Mar)*, 5WW/FM-84/002, Langley AFB, VA, Sep 1984.
- Perrone, Thomas J., *Winter Shamal in the Persian Gulf*, NAVENVPREDRSCHFAC Technical Report TR 79-06, Monterey, CA, Aug 1979.
- Powell, J., and D. E. Pedgley, "A Year's Weather at Termit, Republic of Niger," *Weather*, Vol 24, pp. 247-254, 1969.
- Ramage, C. S., *Monsoon Meteorology, International Geophysics Series, Vol 15*, Academic Press, New York, 1971.
- Ryan, Paul B., *The Iranian Rescue Mission, Why It Failed*, Naval Institute Press, Annapolis, MD, 1985.
- Siraj, Ahmad A., *Aziab Weather*, unknown publisher, AWS Technical Library, Scott AFB, IL, 1980.

Soltani, Ghodratollah (Jim), *The Climate of Iraq and the Arabian Peninsula*, AWS/FM-90/004, Scott AFB, IL, Sep 1990.

Soltani, Ghodratollah (Jim), *The Climate of Iran*, AWS/FM-90/003, Scott AFB, IL, Sep 1990.

Stewart, Dorothy A., Oskar M. Essenwanger, and Larry J. Levitt, *Atmospheric Conditions in the Middle East*, Technical Report RR-85-3, U.S. Army Missile Command, Redstone Arsenal, AL, Jun 1985.

Study of Blowing Dust in the 19th Weather Region, (North Africa - Middle East), AWS/TR 105-49, Scott AFB, IL, Feb 1945.

A Study of Windborne Sand and Dust in Desert Areas, Technical Report ES-8, U.S. Army Natick Laboratories, Natick, MA, Aug 1963.

Vojtesak, Michael J., et al., *SWANEA (Southwest Asia-Northeast Africa). A Climatological Study; Volume II--The Middle East Peninsula*, USAFETAC/TN-91/002, USAF Environmental Technical Applications Center, Scott AFB, IL, Feb 1991.

Walker, Alta S., "Eolian Landforms," *Geomorphology From Space, A Global Overview of Regional Landforms*, pp. 447-520, NASA, 1986.

Weather in the Indian Ocean to Latitude 30° S and Longitude 95° E Including the Red Sea and Persian Gulf, Part 1, Red Sea, NAVENVPREDRSCHFAC Technical Bulletin 80-02, April 1980, reprint from *Weather in the Indian Ocean*, British Meteorological Office, 1940-1944.

Whithead, Michael E., *Sandstorm in the Arabian Sea*, NEPRF Technical Bulletin 80-07, NAVENVPREDRSCHFAC, Monterey, CA, Aug 1980.

DISTRIBUTION

USAF/XOW, Washington, DC 20330-5054	1
AWS/DO/RM/PM/SC/XT/XTX/IG/LN, Scott AFB, IL 62225-5008.....	1
OSAF SS, Rm 4C1052, Pentagon, Attn: Wea Staff, Wash DC 20330-6560	1
OL-A, AFCOS, Ft Ritchie, MD 21719-5010	1
CSTC/WE, PO Box 3430, Onizuka AFB, CA 94088-3430	1
OD-4/DX, Onizuka AFB, CA 94088-3430	1
Det 4, HQ AWS, Weather Warrior Center, Hurlburt Fld, FL 32544-5000	1
Det 5, HQ AWS, Wea Tng Material Devel Ctr, Keesler AFB, MS 39534-5001	1
Det 9, HQ AWS, PO Box 12297, Las Vegas, NV 89112-0297	1
1SSD/WE (Stop 77), Buckley ANG Base, Aurora, CO 80011-9599	1
OL-B, HQ AWS, Hanscom AFB, MA 01731-5000	1
OL-E, HQ AWS, Ft Leavenworth, KS 66027-5310	1
SSD/MWA, PO Box 92960, Los Angeles, CA 90009-2960	1
OL-H, HQ AWS, Ft Huachuca, AZ 85613-7000	1
OL-I, HQ AWS, Ft Monroe, VA 23651-5000	1
AFGWC/DO, 106 Peacekeeper Dr., STE2N3, Offutt AFB, NE 68113-4039	3
AFGWC/SY, 106 Peacekeeper Dr., STE2N3, Offutt AFB, NE 68113-4039	2
AFGWC/DOF, 106 Peacekeeper Dr., STE2N3, Offutt AFB, NE 68113-4039	5
AFGWC/DOM, 106 Peacekeeper Dr., STE2N3, Offutt AFB, NE 68113-4039	5
USAFETAC, Scott AFB, IL 62225-5438	6
PACAF/DOW, Hickam AFB, HI 96853-5000	3
11WS/DON, 6900 9TH St, Ste 205, Elmendorf AFB, AK 99506-2250	1
20WS/DON, APO San Francisco 96328-5000	1
30WS/DON, APO San Francisco 96301-0420	1
USAFE/WX, Unit 3135, Box 15, APO AE 09094-5000	3
7WS/DON, APO AE 09403-5000	1
28WS/DON, APO AE 09127-5000	1
31WS/DON, APO AE 09136-5000	1
HQ SAC/DOW, 901 SAC Blvd, Ste M138, Offutt AFB, NE 68113-5340	3
15AF/DCW, March AFB, CA 92518-5000	1
ATC/DOTW, Randolph AFB, TX 78150-5000	1
8AF/DOW, Barksdale AFB, LA 71110-5002	1
2AF/DOW, Beale AFB, CA 95903-5000	1
SPACECOM/DOW, Peterson AFB, CO 80914-5000	3
AFMC/DOW, Wright-Patterson AFB, OH 45433-5000	1
AFSC/DOW, Andrews AFB, MD 20334-5000	1
TAC/DOW, Langley AFB, VA 23665-5000	7
1WS/DON MacDill AFB, FL 33608-5000	1
9AF/WE, Shaw AFB, SC 29152-5000	1
5WS/DON, Ft McPherson, GA 30330-5000	1
12AF/WE, Bergstrom AFB, TX 78743-5000	1
MAC/XOW, Scott AFB, IL 62225-5008	3
438MAW/WXF, McGuire AFB, NJ 08641-5002	1
60MAW/WXF, Travis AFB, CA 94535-5986	1
3350 TCHTG/TTGU-W, Stop 62, Chanute AFB, IL 61868-5000	2
3395 TCHTG/TTKO-W, Keesler AFB, MS 39534-5000	2
AFIT/CIR, Wright-Patterson AFB, OH 45433-6583	1
USCINCPAC (J37), Box 13, Camp H.M. Smith, HI 96861-5025	1
NAVOCEANCOMDET, Federal Building, Asheville, NC 28801-2723	1
NAVOCEANCOMDET, Patuxent River NAS, MD 20670-5103	1

NAVOCEANCOMFAC, NAS North Island, San Diego, CA 92135-5130	1
COMNAVOCEANCOM, Code N312, Stennis Space Ctr, MS 39529-5000	1
COMNAVOCEANCOM, Code N332, (Capt Brown), Stennis Space Ctr, MS 39529-5001	1
NAVOCEANO, (Rusty Russum), Stennis Space Ctr, MS 39522-5001	2
NAVOCEANO, Code 9220 (Tony Ortolano), Stennis Space Ctr, MS 39529-5001	1
Maury Oceanographic Library (NOC), Code XJL, Stennis Space Ctr, MS 39529-5001	1
FLENUMOCEANCEN, Monterey, CA 93943-5006	1
NOARL West, Monterey, CA 93943-5006	1
Naval Research Laboratory, Code 4323, Washington, DC 20375	1
Naval Postgraduate School, Chmn, Dept of Meteorology, Code 63, Monterey, CA 93943-5000	1
Naval Eastern Oceanography Ctr (Clim Section), U117 McCady Bldg, Norfolk NAS, Norfolk, VA 23511-5000	1
Naval Western Oceanography Ctr, Box 113, Attn: Tech Library, Pearl Harbor, HI 96860-5000	1
Naval Oceanography Command Ctr, COMNAVMAR Box 12, FPO San Francisco, CA 96630-5000	1
Naval Oceanography Command Ctr, Box 31, USNAVSTA, FPO New York, NY 09540-3000	1
Pacific Missile Test Center, Geophysics Division, Code 3253, Pt Mugu, CA 93042-5000	1
HQ NATO Staff Meteorological Officer IMS/OPS APO AE 09724	1
NOAA/MASC Library MC5, 325 Broadway, Boulder, CO 80303-3328	2
OFCM, Suite 900, 6010 Executive Blvd, Rockville, MD 20852	1
NOAA Library-EOC4WSC4, Attn: ACQ, 6009 Executive Blvd, Rockville, MD 20852	1
NOAA/NESDIS (Attn: Nancy Everson, E/RA22), World Weather Bldg, Rm 703, Washington, DC 20233	1
NOAA/NESDIS (Attn: Capt Pereira, E/SP1), FB #4, Rm 0308, Washington, DC 20233-0001	1
NGDC, NOAA, Mail Code E/GC4, 325 Broadway, Boulder, CO 80303-3328	1
Armed Forces Medical Intelligence Agency, Info Svcs Div., Bldg 1607, Ft Detrick, Frederick, MD 21701-5004	1
PL OL-AA/SULLA, Hanscom AFB, MA 01731-5000	1
Atmospheric Sciences Laboratory (SLCAS-AT-AB), Aberdeen Proving Grounds, MD 21005-5001	1
Atmospheric Sciences Laboratory (SLCAS-AS-I 310-2c), White Sands Missile Range, NM 88002-5501	1
TECOM Atmos Sci Div, Attn: AMSTE-TC-AA (MacBlain), White Sands Missile Range, NM 88002-5504	1
Army Missile Command, ATTN: AMSMI-RD-TE-F, Redstone Arsenal, AL 35898-5250	1
Army Test & Eval Cmd, ATTN: AMSTE-TC-AM (RE) TCOM Met Team, Redstone Arsenal, AL 35898-8052	1
Commander and Director, U.S. Army CEETL, Attn: GL-AE, Fort Belvoir, VA 22060-5546	1
6510 TESTW/TSTL, Edwards AFB, CA 93523-5000	1
RL/DOVL, Bldg 106, Griffiss AFB, NY 13441-5700	1
AFESC/RDXT, Bldg 1120, Stop 21, Tyndall AFB, FL 32403-5000	1
Technical Library, Dugway Proving Ground, Dugway, UT 84022-5000	1
NWS W/OSD, Bldg SSM C-2 East-West Hwy, Silver Spring, MD 20910	1
NWS Training Center, 617 Hardesty, Kansas City, MO 64124	1
NCDC Library (D542X2), Federal Building, Asheville, NC 28801-2723	1
NIST Pubs Production, Rm A-405, Admin Bldg, Gaithersburg, MD 20899	1
JSOC/Weather, P.O. Box 70239, Fort Bragg, NC 28307-5000	1
75th RGR (Attn: SWO), Ft Benning, GA 31905-5000	1
HQ 5th U.S. Army, AFKB-OP (SWO), Ft Sam Houston, TX 78234-7000	1
CC/AZSB-GTFD(AH-64CSM-ATTAC), Ft Campbell, KY 42223-5000	1
DTIC-FDAC, Cameron Station, Alexandria, VA 22304-6145	2
AUL/LSE, Maxwell AFB, AL 36112-5564	1
AWSTL, Scott AFB, IL 62225-5438	50